PREPARATION AND DIELECTRIC PROPERTIES AT MHz AND GHz FREQUENCIES OF CERAMICS IN THE SYSTEM Al_2O_3-SrO-TiO_2

by

SANTOSH KUMAR SAHOO

MATERIALS SCIENCE PROGRAMME

INDIAN INSTITUTE OF TECHNOLOGY KANPUR

December, 1999

PREPARATION AND DIELECTRIC PROPERTIES AT MHz AND GHz FREQUENCIES OF CERAMICS IN THE SYSTEM Al_2O_3-SrO-TiO_2

A Thesis Submitted

in Partial Fulfillment of the Requirements

for the Degree of

Master of Technology

by

SANTOSH KUMAR SAHOO

to the

MATERIALS SCIENCE PROGRAMME

INDIAN INSTITUTE OF TECHNOLOGY KANPUR

DECEMBER, 1999

CERTIFICATE

It is certified that the work contained in this thesis entitled " Preparation and Dielectric Properties at MHz and GHz Frequencies of Ceramics in the System Al_2O_3-SrO-TiO_2", by Santosh Kumar Sahoo, has been carried out under my supervision and that this work has not been submitted elsewhere for any degree .

Dr. D.C. Agrawal
Professor
Materials Science Programme,
Indian Institute of Technology,Kanpur
21 December,1999

Dedicated to

My Parents

Acknowledgement

I derive my esteemed pleasure in expressing my deep sense of gratitude to Professor Dinesh Chandra Agrawal for suggesting the problem, supervising the work and being a potential source of inspiration at each stage of this investigation .I am deeply indebted to him for his inspiring guidance, meticulus attention and constructive critism .The completion of this thesis has been possible, only due to his intellectual support .I hope that his work and his example would continue to enspire me during my entire career in future .

I am extremely grateful to Prof. Jitendra Kumar for allowing me to have free access to impedance analyzer for dielectric constant and TCF measurement .

I sincerely appreciate the companionship of my labmates Rasmi, Sarika, Banashree, Amit, Dubey and also exlabmates Atanuda and soumen for providing a better work culture inside the lab. My special thank to Mr. Vishwa Vandhu Mishra .

I wish to thank all my oriya friends Pratap, Manoj, Chand, Suprem, Baroda, Alok, Debajyoti, Tanmaya, Pravanjan, Pabitra, Girija, Rashmi, Sangeeta, Sasmita, Jyotirmayee, Biranchi, Ullas Bhai, Sukant Bhai , Subash Bhai, Nandi Bhai, Pramod Bhai, Ranjan, Mahapatra Sir, and my class mates Manoj, Vineet, Murali Krishna, Mini, Srikanth, Ramanujam, Pandey,Saibaba and my neighbouring lab mates Anshuman, Akash, D.K, Debasish, Gopal, Balasubramanyam who made my stay in the campus cherishable one.

I also express my sincere thanks to all the staffs and members of MSP and ACMS for their help and cooperation towords me .

The unbreakable patience of my family members and their silent support were always a source of inspiration. I am indebted to my Kailash dada and my brother(Basanta) who shoulder all my responsibilities when I was away from home .

Santosh Kumar Sahoo.

IIT-Kanpur .

Abstract

Ceramics in the system $(1-x)Al_2O_3-xSrTiO_3$ with x=0.01,0.02,0.05,0.08 (by weight) have been prapared and characterized with respect to their density, phases, microstructure and dielectric properties. Only Al_2O_3 and $SrTiO_3$ phases are found in the calcined powders. Two additional phases $SrAl_{12}O_{19}$ and $SrTi_3Al_8O_{19}$, are also observed in the sintered samples. High density (95 to 96%) is obtained for the composition 5wt% $SrTiO_3$. Changes in the lattice parameters of Al_2O_3 and $SrTiO_3$ with composition indicate that some solid solution formation is occuring. The dielectric constant of the ceramics is found to be between 9.5 to 10.5. The temperature co-efficient of resonant frequency (TCF) of 1wt% sample is –43 and changes to +11.3 for the 8wt% sample. Thus it appears feasible to design composition with near zero TCF in the system. Co-axial resonator devices prepared using the 1wt% composition have a quality factor of 800 at 1.8 GHz which is in the acceptable range for the co-axial resonator devices.

Contents

List of Figures

List of Tables

CHAPTER-1

Introduction

1.1 General

In recent years there has been a rapid development in microwave telecommunication technology for applications such as car telephone systems, portable telephones and satellite broadcasting receivers[1]. Microwaves are also used in defence systems such as radar, sonar and weapon guidance systems. Other applications are commercial systems like data communications and video/audio communications.

Now a days reduction in the cost and size are the main parameters in the designing of microwave circuits. The most important components used in microwave circuits for applications such as broadcasting via satellite and mobile telephones are resonators and filters. Till 1980's these components used to be large cavity resonators made of invar or copper. Invar wave guide is used in applications where high temperature stability is required and lower cost copper wave guide is used in applications where low temperature stability can be tolerated. The size of these wave guide resonators is not compatible with strip line integrated circuits[2].

Recently microwave telecommunication technology has advanced by miniaturization of components of microwave circuits which is mostly in terms of miniaturization of resonators, through the development of microwave dielectric ceramics[3]. A high dielectric constant (ε_r), a high quality factor (Q), and a zero temperature co-efficient of resonant frequency (τ_f) are the dielectric properties

required for a microwave resonator material. Dielectric resonators are suitable for the development of microwave systems as they offer the possibility of size reduction for microwave components (size $\alpha 1/\sqrt{\varepsilon_r}$, where ε_r is relative permittivity

of dielectric materials)[4]. All the requirements high 'Q', high temperature stability and small dimensions can only be met by the use of dielectric ceramics resonators. The quality of a resonator depends upon the dielectric properties of the material at microwave frequency.

1.2 DIELECTRIC RESONATOR

A dielectric resonator is made of a low loss, high dielectric constant and temperature stable ceramic material in a regular geometric form like disc, co-axial, spherical etc. For a practical resonator the cylindrical (disc type) structure is more preferred than other type of structures because cylindrical resonators do not have a large number of degenerate modes and are easier to fabricate and mount in microwave circuits. The dielectric properties of ceramic materials to be considered for use in dielectric resonators in microwave circuits are[3],

(a) high unloaded quality factor (Q_o)

(b) low temperature co-efficient of resonant frequency (τ_f)

(c) high dielectric constant (ε_r)

1.2.1 PARAMETERS OF DIELECTRIC MATERIALS

QUALITY FACTOR (Q)

The quality factor 'Q' is an important parameter for every dielectric material which is to be used for electronic device applications. The quality factor 'Q' of a dielectric resonator is defined as[5],

$Q = f_r/\Delta f = \omega/\Delta\omega$

where 'f_r' is the resonant frequency and 'Δf' is the band width between the frequencies $f_r - \Delta f/2$ and $f_r + \Delta f/2$ for which the electric and magnetic energy is reduced to $1/\sqrt{2}$ times of its value at resonant frequency 'f_r' ($\omega = 2\pi f$).

The quality factor is also written as,

$$Q = \frac{2\pi \ \max imum\ energy\ stored}{energy\ dissipated\ per\ cycle}$$

Which gives,

$$Q = \frac{X_l}{R} = \frac{2\pi f_r L}{R}$$

Where X_L = Reactance

L = Inductance

R= Resistance

TEMPERATURE CO-EFFICIENT OF RESONANT FREQUENCY (τ_f)

The temperature co-efficient of dielectric constant is given by,

$$TCK = \frac{1}{K}\frac{\partial K}{\partial T}$$

where '∂K' is the change in dielectric constant (K) due to a small change in temperature '∂T'.

The temperature co-efficient of resonant frequency is defined by[6],

$$TCF = \frac{1}{f_r}\frac{\partial f_r}{\partial T}$$

TCF and TCK are related[7],

$$TCF = -\frac{TCK}{2} - \alpha \quad ,$$

Since TCC = TCK +α, we get

$$TCF = -\frac{1}{2}\left(TCC + \alpha\right)$$

where α = co-efficient of thermal expansion and 'TCC' is the temperature co-efficient of capacitance

DIELECTRIC CONSTANT (ε_r)

The dielectric constant of a dielectric material is defined by,

$$Dielectric\ Constant\,(\varepsilon_r) = \frac{Capacitance\ of\ the\ capacitor\ with\ dielectric\ material}{Capacitance\ of\ the\ capacitor\ without\ dielectric\ material} = \frac{C}{Co}$$

.

At present two types of resonators are used. These are co-axial λ/4 resonators for use in the frequency range upto 3GHz and solid dielectric resonators for use in the frequency range upto 30 GHz [6]. The quality factor (Q) of co-axial

resonators is usually limited to values < 1500 due to finite conductivity of the electrode material. But in case of solid dielectric resonator there is no electroding. So in this case the quality factor is limited by the material's quality factor. The material's quality factor is the determining property for the behaviour of oscillators and filters. In order to produce low noise oscillators and narrow band width microwave filters with low dielectric loss, the resonators should posses a high quality factor. So solid dielectric resonator is more preferable over co-axial resonator.

The dimension (L) of a co-axial resonator is given by[6],

$$L=\lambda o/4\sqrt{\varepsilon_r}$$

The high dielectric constant (ε_r) ceramics are used to reduce the size of the microwave circuit components. The size of the resonator determines the resonant frequency of the material. Now the development of large scale integration (LSI) and very large scale integration (VLSI) has promoted the production of multilayer substrates in order to reduce size[8], higher integration density and better reliability for electronic systems. A low K dielectric ceramic is also used as a substrate because it reduces the time delay of electronic signals during propagation through the conductor, which is fabricated on the substrate[9].

Low K dielectric ceramics are used in applications such as multilayer substrates in insulating the conductors in hybrid circuits[7] as low permittivity minimises coupling between components on substrate surface .

1.2.2 APPLICATIONS OF DIELECTRIC RESONATOR

(i) Frequency stabilization of oscillator

Dielectric resonators can be used to make compact frequency-stable oscillators with high quality factor and low noise. Dielectric resonators can also be used to stabilize voltage controlled oscillators that can be tuned in a wide range of frequency. Figure (1.1) shows the schematic circuit diagram of the " out door " unit of a receiver for 12 GHz satellite television in which the oscillator is stabilized by a dielectric resonator. Figure (1.2) shows the cross section of DR-oscillator for high capacity digital radio system[6].

(ii) Microwave filters with dielectric resonator

The high unloaded quality factor of dielectric resonators makes it possible to produce filters with narrow bandwidth and low loss. Figure (1.3) and fig (1.4) show the application of dielectric resonators as band pass filters[6].

1.2.3 APPLICATIONS OF CO-AXIAL RESONATOR

(i) Stabilization of oscillators

In the transmitting branch as well as in the receiving branch, channel tunning occurs by a voltage controlled oscillator. The figure (1.5) shows the circuit diagram of the radio frequency part of a cord less telephone in which the voltage controlled oscillator is stabilized by co-axial resonator[6].

(ii) Microwave filters

The band pass filters in the transmitting and receiving branch as well as the duplex filter on the antenna side for de-coupling transmission and receiving band can be produced by ceramic co-axial resonator[6] and is shown in figure 1.6.

(iii) Dielectric Substrates:

Microwave ceramics with high ε_r can be used as MIC substrates[6].

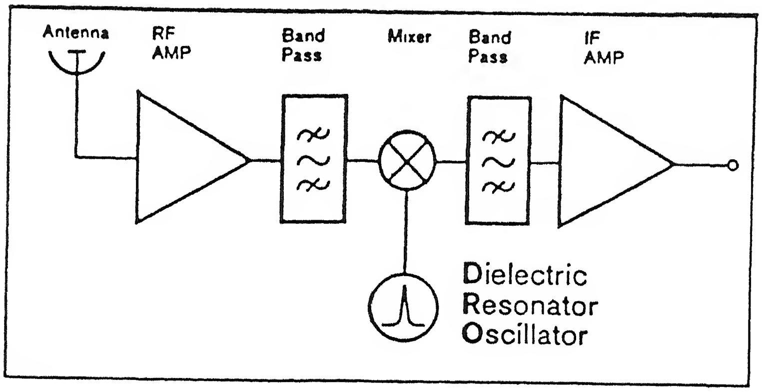

Figure 1.1: Schematic circuit diagram of the "out door" unit of a receiver for 1
GHz Satellite television [6] .

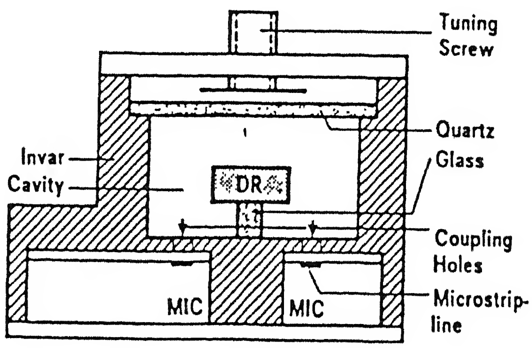

Figure 1.2: Cross section of DR-oscillator for high capacity digital radio syste

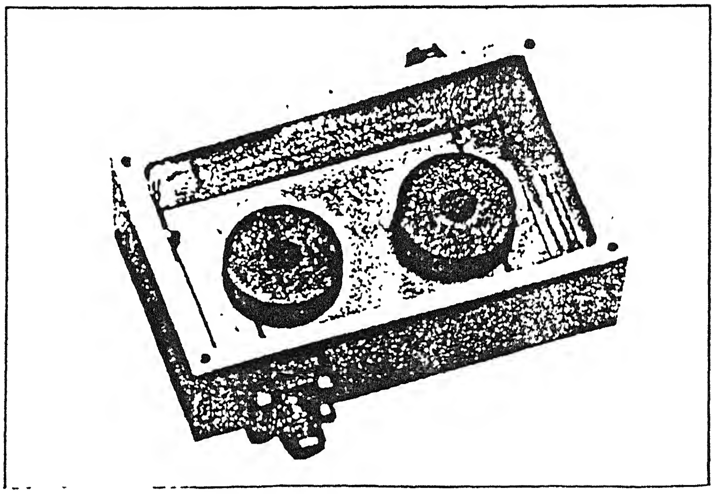

Figure 1.3: Two pole band pass filter with dielectric resonators on a MIC substra

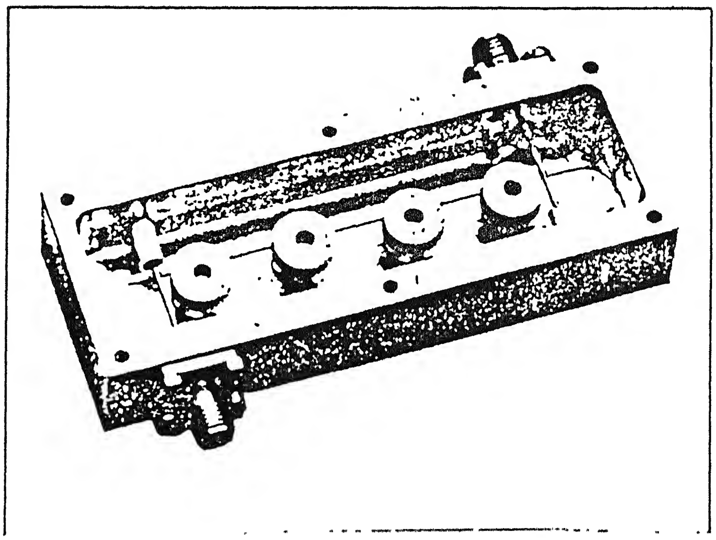

Figure 1.4: Four pole band pass filter with dielectric resonators on a MIC substra

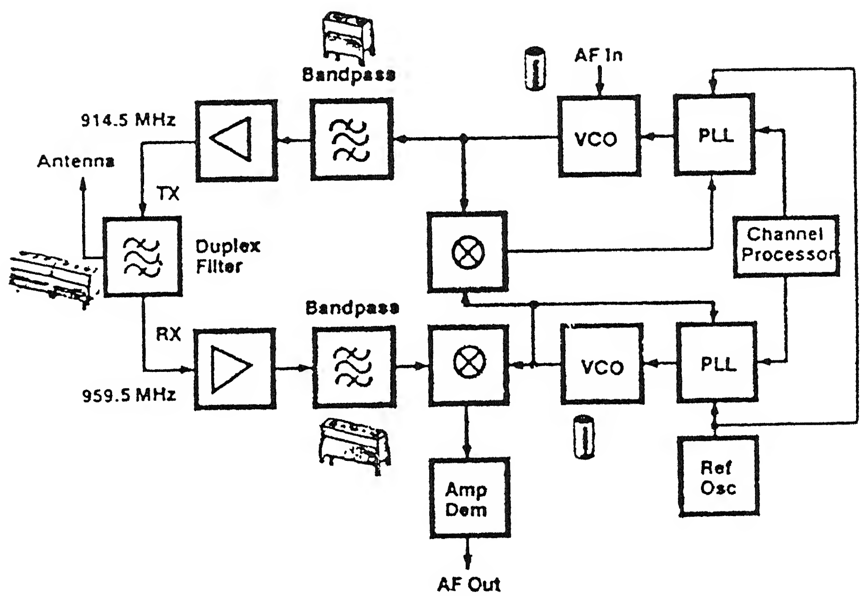

Figure 1.5: Circuit diagram of the radio frequency part of a cordless telepho which the voltage controlled oscillator is stabilized by co-axial resonator 6

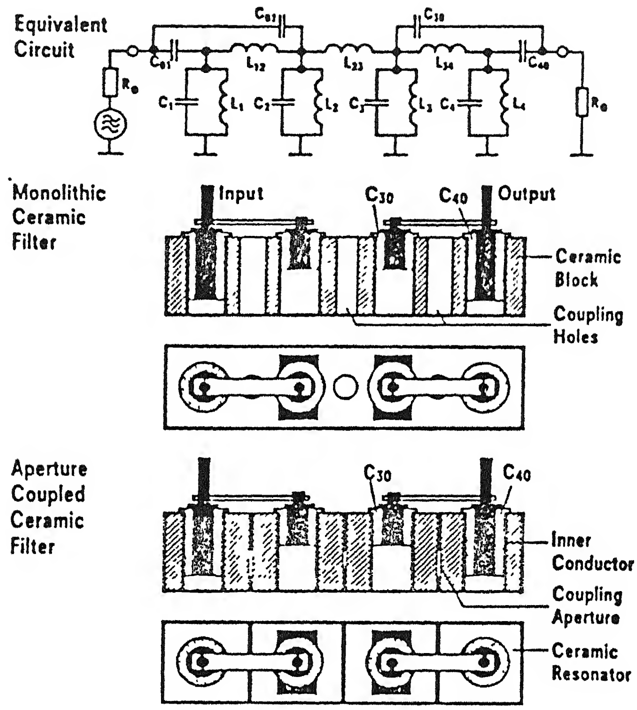

Figure 1.6: Microwave filters made of ceramic co-axial resonators [6]

1.3 DIELECTRIC RESONATOR MATERIALS

Some important microwave dielectric ceramics used in dielectric resonator are given in the table below[6].

TABLE: 1.1 Dielectric properties of some important microwave dielectri ceramics.

Ceramic	ε_r	TCF (ppm/°k)	Q	
			2 GHz	20 GHz
$Ba_2Ti_9O_{20}$	40	2	15,000	2000
$Zr_{0.8}Sn_{0.2}TiO_4$	38	0	15,000	3000
$BaTi_u[(Ni_xZn_{1-x})_{1/3}Ta_{2/3}]_{1-u}O_3$	30	-3 ...3	26,000	5000
$Ba[Sn_x(Mg_{1/3}Ta_{2/3})_{1-x}]O_3$	25	~ 0	>40,000	10,000
Nd_2O_3-BaO-TiO_2-Bi_2O_3	~90	~0	3,000	--

1.3.1 $MgTiO_3$-$CaTiO_3$ System

TABLE -1.2 Dielectric Properties of $MgTiO_3$ and $CaTiO_3$ Ceramics at 7 GHz.

	ε_r	Q	τ_f
$MgTiO_3$	17	22,000	-45
$CaTiO_3$	170	1800	+800

The temperature co-efficient of resonant frequency exhibits large negativ and positive values for the Mg and Ca titanates respectively[4]. For practica applications a mixed composition of approximately $(Mg_{0.95}Ca_{0.05})TiO_3$ is u. ally selected to yield τ_f ~0.

1.3.2 $Ba_2Ti_9O_{20}$ and $BaTi_4O_9$ systems

Barium titanate ceramics in the system $Ba_2Ti_9O_{20}$-$BaTi_4O_9$ [4] have relative

permittivities ~ 40 are comparable with those of $(Zr,Sn)TiO_4$ ceramics and Q values at 4 GHz are typically 8000. Such materials have proved suitable for practical applications at 11 GHz. The properties of $Ba_2Ti_9O_{20}$-$BaTi_4O_9$ ceramic also appear to be sensitive to the presence of trace element contaminants and th furnace atmosphere during cooling after sintering.

1.3.3 $(Zr,Sn)TiO_4$ System

Zirconium titanate based ceramics have been recognized as temperatur stable dielectrics[4]. The addition of Sn to form solid solution of $(Zr,Sn)TiO_4$ lead to stabilization of high temperature form and the enhancement of the dielectric Q value. Good quality ZTS ceramics can be prepared by the mixed oxide and chemical route. The dielectric Q-value depends upon the cooling rate. If the cooling rate is slow, then the Q-value is more. If the cooling rate is rapid, then the Q-value is less. The variation of TCF and Q-factor of ZTS ceramics with Sn content are given in figure (1.7) and fig (1.8)[6].

1.3.4 Complex Perovskites

Dielectric resonators with a complex perovskite structure have permittivities in the range 25-30 and Q-values in the range 10,000-40,000 at 10 GHz[6]. $Ba(Zn_{1/3}Ta_{2/3})O_3$ and $Ba(Mg_{1/3}Ta_{2/3})O_3$-$BaSnO_3$ are the two main systems in this perovskite system. Perovskite dielectric ceramics are sensitive to purity and composition and elimination of 2nd phase is essential to attain highest Q - values.

1.3.5 BaO-RE_2O_3-TiO_2 System

The demand for microwave dielectric ceramics of smaller size and higher relative permittivity stimulated research into a new family of materials based on BaO-M_2O_3-TiO_2, where 'M' is a rare earth species[4]. Kolar investigated the

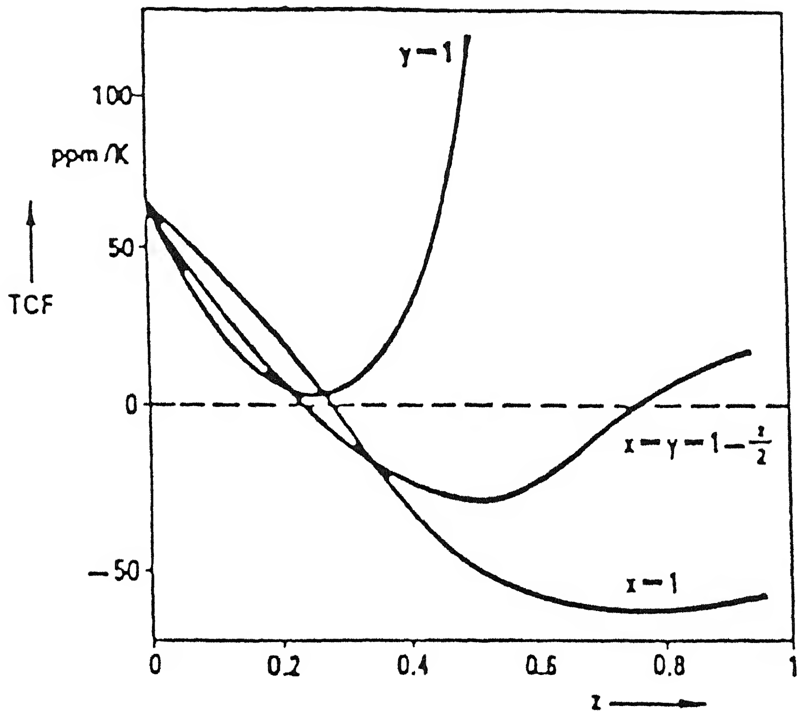

Figure 1.7: Temperature coefficient of resonant frequency of ZTS ceramics as fu
content [6]

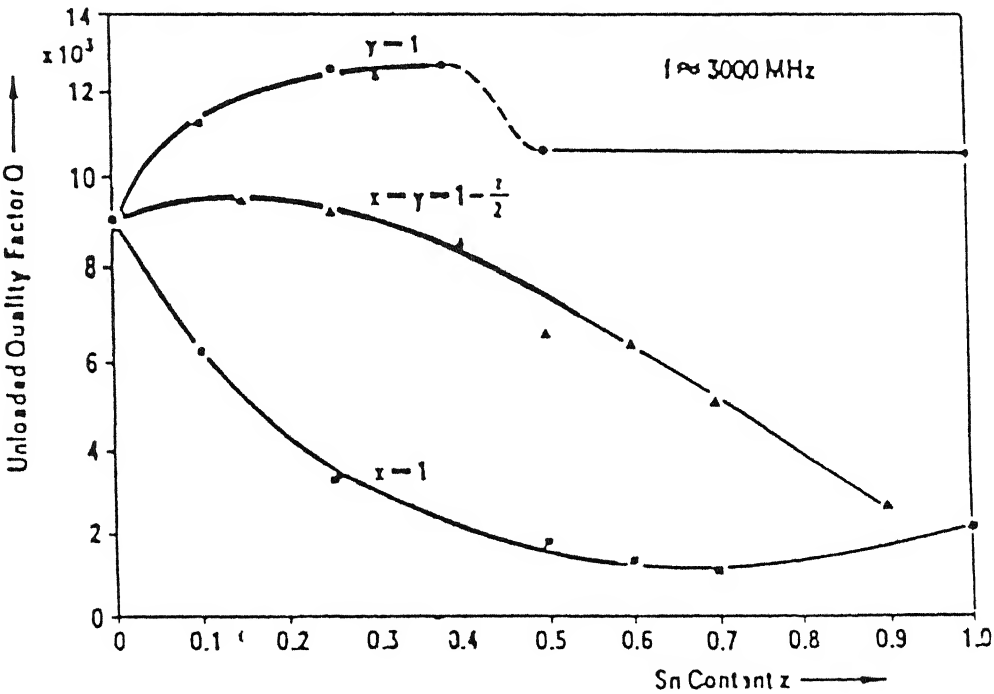

Figure 1.8: Quality factor of ZTS dielectric resonator as a function of Sn content[6

system $BaO-Nd_2O_3-TiO_2$ and found that the relative permittivity is up to 92 and Q-value up to 3,000 at 1MHz. The best properties were achieved for these ceramics with compositions 1:1:5 and 1:1:4 ($BaO : Nd_2O_3 : TiO_2$). The other dielectric ceramics in this system are $BaO-Sm_2O_3-TiO_2$, $BaO-La_2O_3-TiO_2$ and $BaO-Bi_2O_3-Nd_2O_3-TiO_2$.

1.4 Statement of the Problem

Alumina is a low dielectric constant ($\varepsilon \sim 10$) low dielectric loss material ($\tan\delta$ 1-10x10^{-4} at 1-10 GHz). It is commonly used as a substrate for microwave circuits. However for application to microwave components (e.g resonators /filters) its temperature stability is a limiting factor. The temperature co-efficient of resonant frequency of Al_2O_3 is ~(-67 -82) ppm/^{o}C, which for resonator applications is unacceptable. To achieve a near zero temperature co-efficient, in Al_2O_3 based dielectrics, a suitable second phase is required. $SrTiO_3$ has a large temperature co-efficient of resonant frequency ~ +1700 ppm/^{o}C which is of opposite sign[10] to that of Al_2O_3. Thus by having a two phase (Al_2O_3 and $SrTiO_3$) ceramic in suitable weight ratios, it is expected that a near zero temperature co-efficient of resonant frequency material may be obtained.

Perry and Alderton[11] have reported the phases obtained in $Al_2O_3-SrTiO_3$ samples of different compositions (3 to 23 wt% $SrTiO_3$). They found that while Al_2O_3 was the main phase in the 3 and 10 wt % $SrTiO_3$ compositions, in the higher composition the main phase was $SrO.6Al_2O_3$. No significant amount of $SrTiO_3$ phase was found in any composition. The authors suggested that the temperature stabilization suggested by Atlas et al may be due to $SrO.6Al_2O_3$ rather than due to $SrTiO_3$. The dielectric constant and TCF of a multiphase ceramic can be predicted reasonably - by using suitable rules of mixture if the corresponding data for the pure phases is available. The values of the dielectric constants and TCF's of Al_2O_3 and $SrTiO_3$ are known but that of $SrO.6Al_2O_3$ have not been reported to the best of

our knowledge. In order to decide on the range of composition which might yield the desired values (dielectric constant =10, TCF=0) one has there fore to make some assumptions. We have assumed that the values of these parameters for $SrO.6Al_2O_3$ are not too different from those for $SrTiO_3$. Based on this assumption we have selected the composition range Al_2O_3 1 to 8 wt% $SrTiO_3$ for investigation. The aim of the investigation is to prepare samples in this composition range with good sintered density and to characterize them with regard to their phases, microstructure and dielectric properties. It is also planned to make a device out of the suitable composition and measure its performance.

CHAPTER-2

Experimental Procedure

2.1 Sample Preparation

The specifications of the starting powders are given in Table-2.1. All the three powders Al_2O_3, TiO_2 and $SrCO_3$ were weighed separately and kept inside an oven for 24 hours at 120°C. After removing from the oven, the individual powders were weighed again. The losses due to the adsorbed moisture are given in Table:1. Weighed amount of each individual dried powder was further heated separately in a furnace at 1000°C for 4 hours. The weight loss on ignition was obtained and is also given in Table:1. No decomposition of $SrCO_3$ occurs at 1000°C .

TABLE :2.1 The specifications of the starting powders .

S. No	Powder	Supplier	Purity	Molecular Weight	Density	Wt loss On drying	Wt loss On heating dried powder to 1000°c
1.	Al_2O_3	Sumitomo Chemical Co.Tokyo	99.9 %	101.96	3.987	0.3	0.36
2.	TiO_2	Aldrich Chemical Company,Inc UK	99+%	79.90	3.900	0.3	0.8
3.	$SrCO_3$	New India Chemical Enterprises,Kochi 682024	----	147.63	3.700	0.35	3.25

2.2 Batch Preparation, Calcination and Pressing

The samples were prepared to yield the composition $(1-x)Al_2O_3-xSrTiO_3$ with different weight fractions (x=0.01,0.02,0.05,0.08). The calculation of the required amounts of each powder for a particular composition and for a particular batch is given in Appendix A. For the preparation of a particular batch with a particular composition, the calculated amounts of the starting powders were taken. These powders were taken in a teflon jar for mixing by ball milling. Alumina balls and propanol were added to this powder for the first ball milling. The weight of the Al_2O_3 balls was four times the weight of the powder. The volume of the propanol was (1.5 x weight of powder) ml. The powder was ball milled for 4 hours at 2.5 speed mark. After ball milling the slury was dried in an oven at 100-110°C.

The dried powder was calcined for 4 hours at two different temperatures (1100°C, 1150°C) separately. The powder was kept in an alumina crucible covered by a perforated Al_2O_3 lid .For calcination the furnace programming was as follows. 7°C/min.from room temp to 900°C, 5°C/min from 900°C to 1100°C, soaking for 4 hours, cooling at 5°C/min from 1100°C to 900°C, 6°C/min from 900°C to room temperature. The weight of material was measured before and after the calcination to confirm that there is no significant weight loss beyond what is expected.

The above calcined powder was ground in mortar pestle for a few minutes. Then the calcined powder was again ball milled with triple distilled water for a second time .The weight of alumina balls and volume of triple distilled water were similar to first ball milling. 2 wt% poly ethylene glycol (PEG) dispersant was added during second ball milling. After ball milling for 4 hours, 1% PVA solution (1 gm of PVA powder in 100 ml of distilled water) was added as a binder to the above slurry. For each gram of powder 1 ml of PVA solution was added. Ball milling was then continued for 15 more minutes. The slurry was then dried in the oven at 100-110°C until nearly dry.

The binderised powder was passed through a seive of size 70-80 mesh to get it in the form of granules. Preweighed amount of powder was pressed into pellets .The amount of powder was about 1.6 gms which produced a sintered pellet 10 mm dia x 5 mm high. The powder was pressed into cylindrical pellets of 12 mm diameter in a hydraulic press using a steel die .The maximum load applied was 20 kN. After 2 minutes of the attainment of maximum load, the load was released .The pressure used was 200 Mpa.

2.3 Binder removal and Sintering

The pressed pellets were heated in a furnace from room temperature to 600°C at 3°C/min, held for 3 h for the removal of binder and then cooled from 600°C to100°C at 5°C/min. After removal of the binder the pellets were placed in the furnace for sintering. The pellets were heated from room temperature to 900°C at 7°C/min, from 900°C to 1400°C at 5°C/min. and held for 2 hours. After this cooling was done from 1400°C to 900°C at 5°C/min, and from 900°C to 200°C at 6°C/min.

2.4 CHARACTERISATION

2.4.1 Density and Phases

The density of the sintered samples were calculated by measuring the diameters and the heights and masses of the pellets .The various crystalline phases present in the calcined powders and also in the sintered samples were determined by x-ray powder diffraction using a monochromatic Cukα radiation.

2.4.2 Dielectric Properties

For dielectric constant ε_r and TCF (τ_f) measurements at 12 MHz, 1mm thick

discs with parallel faces were sliced from pellets using a low speed diamond saw. Both sides of the discs were coated with a silver paste (Eltecks Corporation Bangalore, Code No: 0070). Care was taken to see that the two sides are not shorted .The silver paste was cured at 120°C for 2h in an oven.

The silver coated disc was held in a holder shown in figure 2.1[12] and its capacitance at 12 MHz was measured using an impedance analyzer (Model HP 4192A). The relative permittivity was calculated using the formulae,

$$\varepsilon_r = \frac{4Ct}{\pi \varepsilon_o d^2}$$

where ε_o is the permittivity of free space (8.85×10^{-12} F/m). 'C' is the capacitance of the disc. 't' and 'd' are the thickness and diameter of the sample respectively .The temperature co-efficient of capacitance (TCC) was also measured with the help of the impedance analyzer. The TCC was measured from room temperature to 70-80°C. It was calculated by the formula given as below.

$$TCC = \frac{1}{C(T_1)} \frac{C(T_2) - C(T_1)}{T_2 - T_1}$$

where $C(T_1)$ and $C(T_2)$ are the capacitances at room temperature T_1 and at a higher temperature T_2 (70-80°C).The temperature co-efficient of resonant frequency (TCF) was calculated by using the relation .

$$TCF = -\frac{1}{2}(TCC + \alpha)$$

where 'α' is the linear co-efficient of thermal expansion .The value of 'α' was taken to be $7 \times 10^{-6}\,{}^{0}C^{-1}$ same as that for α-Al_2O_3 as the amount of the other phase in all samples is very small (<5%).

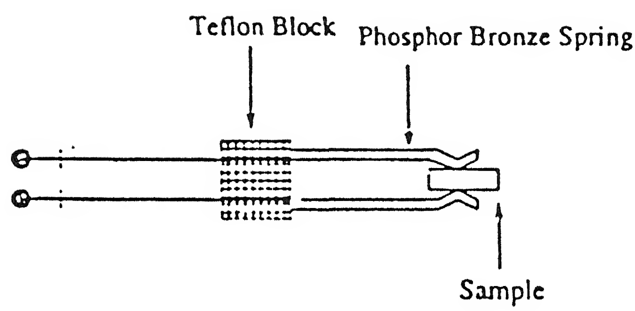

(a)

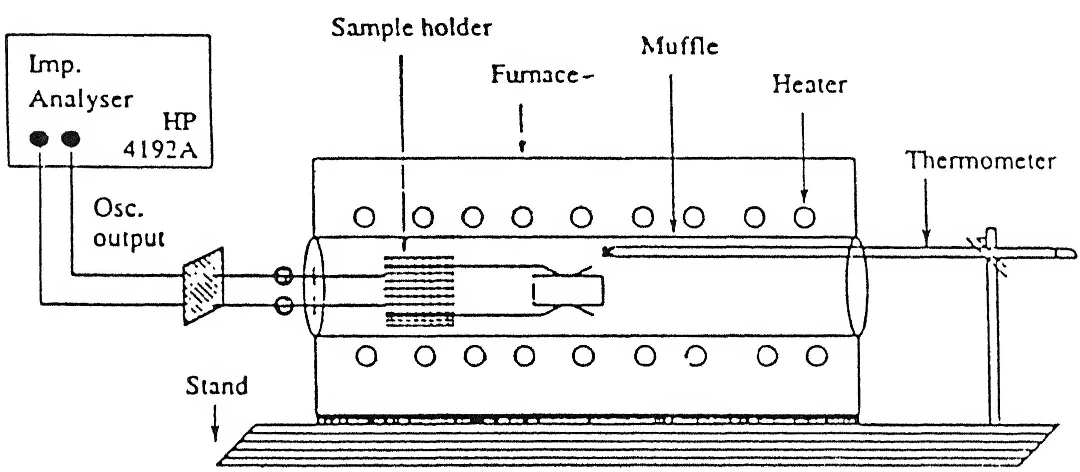

(b)

Figure 2.1: (a) Schematic diagram of sample holder, (b) Schematic arrangement for diele
constant and TCC measurement.[12].

2.4.3 Lattice Parameter Determination

For determination of the lattice parameter only the high angle peaks ($\theta > 60^o$) were used[13] .The peaks were indexed using the standard X-rays data file .The lattice parameters of cubic, hexagonal and rhombohedral systems were determined as follows.

Cubic System ($SrTiO_3$)

In case of cubic system, the general formula used for lattice parameter calculation is,

$$a = \frac{\lambda\sqrt{h^2 + k^2 + l^2}}{2\sin\theta}$$

where is 'a' is the lattice parameter of the system, 'θ' is the angle of diffraction, 'λ' is wave length of x-ray radiation and h k l are the miller indices of the peaks present in the x-ray diffraction pattern. For all angles above 60^o, lattice parameter 'a' values were calculated and then these calculated values were plotted against $\cos^2\theta$. The most accurate value 'a_o' was calculated by extrapolating the plot to a value of $\cos^2\theta \sim 0$, as 'θ' approaches 90^o.

Hexagonal System ($SrAl_{12}O_{19}$)

$SrAl_{12}O_{19}$ has hexagonal crystal structure. From the x-ray diffractogram, first the lattice parameters (a_H, c) of the equivalent hexagonal lattice are determined. The general formulae used for lattice parameter calculation in hexagonal systems are[13],

$$a_H = \frac{\lambda}{\sin\theta}\sqrt{\frac{1}{3}\left(h^2 + hk + l^2\right) + \frac{l^2}{4\left(\frac{c}{a}\right)^2}}$$

$$C = \frac{\lambda}{\sin\theta}\sqrt{\left(\frac{c}{a}\right)^2 \frac{\left(h^2 + hk + k^2\right)}{3} + \frac{l^2}{4}}$$

The accurate lattice parameters in this system were obtained by successive approximation. At first approximate values of a_1 and c_1 of the lattice parameter were calculated. Then the approximate ratio c_1/a_1 was calculated. Again using c_1/a_1, the approximate values of 'a' was calculated for various higher angles. Again plotting 'a`' against $\cos^2\theta$ value, we get a_2 value. Similarly 'c_2' was calculated. Again taking c_2/a_2 ratio c_3 and a_3 values were calculated and so on. The repetition takes place for five successive times before consistent results are obtained.

RhombohedralSystem (Al_2O_3)

The parameters (a_R,α) of rhombohedral system can be determined by using the following formulae[13],

$$a_R = \frac{1}{3}\sqrt{3a_H^{\ 2} + c^2}$$

$$\sin\frac{\alpha}{2} = \frac{3}{2}\sqrt{3+\left(\frac{c}{a_H}\right)^2}$$

where a_H and c are the parameters for hexagonal system. All these are calculated using a programme. The programme used is given in the Appendix E.

2.4.4 Microstructure Studies by SEM

For the study of microstructure, the sintered pellet of different compositions were polished to 0.25μm .The procedure of polishing the samples was as follows.

(a) Polished with SiC(2μm) powder with water on the glass plate for 30 minutes.

(b) Polished with Al_2O_3 (1μm) powder with water on the glass plate for 30 minutes.

(c) Polished with diamond paste (1μm) with hifin fluid on micro polishing cloth for 45 minutes.

(d) Polished with diamond paste (0.25μm) with hifin fluid on micro polishing cloth for 45 minutes.

After polishing, the pellets were cleaned with acetone by ultrasonic dismembrator. After cleaning the pellets were chemically etched with 1HF: $1HNO_3$ solution, then thermally etched at 1300°C for 20 minutes in the furnace. The etched samples were coated with a AuPd coating by using a sputtering machine. Then the samples were examined in a scanning electron microscope (Model JSM 840A, JEOL, Japan).

2.5 Fabrication and Characterization of Co-axial Resonator Devices

Co-axial resonator devices with dimensions given in fig 2.2 were fabricated by dry pressing in a die using about 7 gms of powder for each device .The

sintering was carried out at 1400°C for 2h. The devices were electroded using a silver paste as before on all the four sides, the top surface and the inside hole. The quality factor Q and the resonance frequency f_0 were measured using a network analyzer (Model HP 8719A HP 8720A/B).

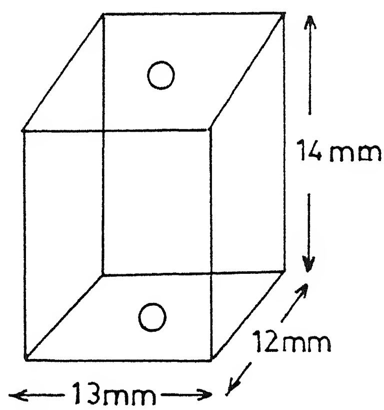

Figure 2.2: Co-axial Resonator Devices with dimensions.

CHAPTER-3

Results and Discussion

3.1 Phases present in the calcined Powders

The various phases present in the calcined powders were determined from X-ray diffractograms using the standard X-ray data for the various possible phases such as Al_2O_3, $SrTiO_3$ and $SrAl_{12}O_{19}$. X-ray data of these phases are given in tables 3.1 to 3.4. This data is combined in ascending 2θ in table 3.5. In the calcined powders of different compositions only two phases Al_2O_3 and $SrTiO_3$ were found. Fig 3.1 shows a diffractograms for calcined powders calcined at 1100°C for 4h.

3.2 Density of the sintered samples

The relative densities of the sintered pellets for different compositions are given in the table 3.6. The theoretical densities for different compositions were calculated assuming that only Al_2O_3 and $SrTiO_3$ phases are present in the amounts taken in the starting batch. The theoretical densities of Al_2O_3 and $SrTiO_3$ are taken to be 3.987 gm/cm^3 and 5.12 gm/cm^3 respectively. The theoretical densities of the batches are also listed in table. Highest densities (95 to 96 %) are obtained for the composition 5wt% $SrTiO_3$ followed by the composition 1wt% $SrTiO_3$. The density obtained for 2wt% $SrTiO_3$ samples is lower which is surprising. The 8wt% $SrTiO_3$ samples sinter poorly to ~ 85% density. A plot between the sintered density and the composition is given in fig 3.2 .It is seen that the highest density (>96 %) is obtained for the 5 % composition and the lowest (<85.7) for the 8 wt%

Table 3.1: Standard X-ray data of Al_2O_3 Phase

10-0173 Wavelength= 1.54056 i

-Al2O3

Aluminum Oxide

Corundum, syn

Rad : CuKa1 λ: 1.5405 Filter: Ni Beta M d-sp

Cut off: Int.: Diffract. I/Icor.: 1.00

Ref: Natl. Bur. Stand. (U.S.), Circ. 539, 9, 3 (1960)

Sys.: Rhombohedral S.G.: R$\bar{3}$c (167)

a 4.758 b c: 12.991 A. C 2.7303

α β γ: Z. 6 mp: 2050

Ref. Ibid

Dx: 3.989 Dm: 4.050 SS/FOM. F_{30}=50(.0188, 32)

εα: 1.7604 ηωβ: 1.7686 εγ: Sign: - 2V:

Ref: Dana's System of Mineralogy, 7th Ed., I, 520

Color: Blue, colorless, yellow
Pattern taken at 26 C. Sample annealed at 1400 C for four hours in an Al2 O3 crucible. Spectroscopic analysis showed <0.1% K, Na, Si; <0.01% Ca, Cu, Fe, Mg, Pb; <0.001% B, Cr, Li, Mn, Ni. Also called ruby. Also called: sapphire Al2 O3 type. Corundum group, corundum subgroup. Also called: alumina. Also called: diamonite PSC. hR10 Mwt: 101.96 Volume[CD]. 254.70

2θ	Int	h	k	l	2θ	Int	h	k	l
25.584*	75	0	1	2	109.833	<1	1	2	11
35.136*	90	1	0	4	111.029	4	3	1	8
37.784*	40	1	1	0	114.126	4	2	2	9
41.683*	<1	0	0	6	116.141	14	3	2	4
43.362*	100	1	1	3	116.630	4	0	1	14
46.183*	2	2	0	2	117.901	8	4	1	0
52.551*	45	0	2	4	120.233	<1	2	3	5
57.518*	80	1	1	6	122.071	4	4	1	3
59.767*	4	2	1	1	124.647	2	0	4	8
61.164*	6	1	2	2	127.731	12	1	3	10
61.344*	8	0	1	8	129.916	4	3	0	12
66.547*	30	2	1	4	131.148	4	2	0	14
68.196*	50	3	0	0	136.162	22	1	4	6
70.357*	2	1	2	5	142.396	4	1	1	15
74.266*	4	2	0	8	145.208	11	4	0	10
76.880*	16	1	0	10	149.287	7	0	5	4
77.227*	8	1	1	9	150.244	14	1	0	16
80.692*	8	2	2	0	152.445	13	3	3	0
83.217*	<1	3	0	6					
84.375*	6	2	2	3					
85.181*	2	1	3	1					
86.375*	6	3	1	2					
86.461*	4	1	2	8					
89.018*	8	0	2	10					
90.662*	4	0	0	12					
91.201*	8	1	3	4					
95.260*	14	2	2	6					
98.407*	2	0	4	2					
101.092	12	2	1	10					
102.788	<1	1	1	12					
103.345	4	4	0	4					
109.522	<1	3	2	1					

Table 3.2: Standard X-ray data of $SrTiO_3$ Phase

35-0734 Wavelength= 1.54056

SrTiO3

Strontium Titanium Oxide

Tausonite, syn

Rad CuKa1 λ: 1.5405 Filter: Ni Beta.M d-sp: Diffractometer

Cut off: Int.: Diffract. I/Icor.: 6.222

Ref: Swanson, H., Fuyat, Natl Bur Stand. (U.S.), Circ. 539, 3 44 (1954)

Sys.: Cubic S.G.: Pm3m (221)

a 3.9050 b: c A. C:

α β. γ Z 1 mp:

Ref. Ibid.

Dx: 5.118 Dm: SS/FOM F_{18}=47(.0182, 21)

Pattern taken at 25 C. Sample from Nat. Lead Co. Spectrographic analysis. <0.01% Al, Ba, Ca, Si, <0.001% Cu, Mg. Perovskite group, loparite subgroup. PSC: cP5. To replace 5-634 and 40-1500. Mwt: 183.52. Volume[CD]: 59.55

2θ	Int	h	k	l
22.783*	12	1	0	0
32.421*	100	1	1	0
39.981*	30	1	1	1
46.183*	50	2	0	0
52.357*	3	2	1	0
57.794*	40	2	1	1
67.803*	25	2	2	0
72.543*	1	3	0	0
77.175*	15	3	1	0
81.721*	5	3	1	1
86.204*	8	2	2	2
95.127*	16	3	2	1
104.150	3	4	0	0
113.609	10	4	1	1
118.585	3	3	3	1
123.827	10	4	2	0
135.416	6	3	3	2
150.136	9	4	2	2

Table 3.3: Standard X-ray data of $SrAl_{12}O_{19}$ Phase

26-0976 Wavelength= 1.54056 i

SrAl12O19

Strontium Aluminum Oxide

Rad Cu λ. 1.5405 Filter: Ni Beta M d-sp:

Cut off: Int.: Diffract. I/Icor.:

Ref: Verstegen. Philips. Eindhoven Netherlands. Private Communication

Sys: Hexagonal S.G: $P6_3/mmc$ (194)

a 5.585 b: c: 22.07 A: C. 3.9517

α: β: γ: Z: 2 mp:

Ref: Ibid.. Private Communication

Dx: 3.985 Dm: SS/FOM. F_{30}=19(.033. 47)

Color: White
Sample K S 250-2. fired from Sr C O3. Mg O and Al (O H)3 at 800 C and 1500 C. Magnetoplumbite type. PSC: hP64. To replace 10-66 Mwt. 715.39. Volume[CD]: 596.18.

2θ	Int	h	k	l	2θ	Int	h	k	l
18.785°	18	1	0	1	52.780°	5	1	1	10
20.027°	30	1	0	2	53.110°	11	2	0	9
24.164°	20	0	0	6	56.402°	3	2	0	10
24.502°	6	1	0	4	57.012°	6	3	0	0
27.249°	4	1	0	5	57.166°	5	3	0	1
31.995°	55	1	1	0	57.754°	4	3	0	2
32.411°	20	0	0	8	58.274°	35	2	1	7
33.026°	16	1	1	2	58.477°	25	0	0	14
33.862°	95	1	0	7	58.681°	5	3	0	3
36.040°	100	1	1	4	59.682°	30	3	0	4
37.120°	7	2	0	0	59.938°	55	2	0	11
37.441°	5	1	0	8	60.197°	6	1	1	12
38.100°	5	2	0	2	60.676°	4	2	1	8
39.133°	40	2	0	3	63.443°	4	2	1	9
40.700°	14	2	0	4	66.333°	4	2	1	10
40.835°	20	0	0	10	66.978°	50	2	2	0
41.284°	5	1	0	9	67.141°	30	3	0	8
42.611°	70	2	0	5					
44.785°	45	2	0	6					
46.333°	2	1	1	8					
49.126°	7	1	0	11					
50.019°	3	2	1	1					
50.136°	3	2	0	8					
51.469°	2	2	1	3					

37-1231 Wavelength= 1.54056

$SrTi_3Al_8O_{19}$

Strontium Aluminum Titanium Oxide

Rad.: CuKa λ. 1.5417 Filter: Graph Mono d-sp. Diffractometer

Cut off: Int.: Diffract. I/Icor.:

Ref. Morgan, P., Rockwell International Science Center, CA. USA, Private Communication, (1985)

Sys.: Monoclinic S.G.: C2/c (15)

a. 22.7020 b: 11.0639 c: 9.7689 A: 2.0519 C 0.8830

α: β. 98 652 γ. Z: 8 mp:

Ref: Morgan, P., Koutsoutis, M., J. Mater. Sci. Lett., 4, 321 (1985)

Dx: 4.114 Dm: SS/FOM. F_{30}=12(.040, 64)

Color: White
Coprecipitation and firing at 1400-1600 C. Cell constants refined from higher angle lines with coincident hkl values with isotypes Ca Ti3 Al8 O19 and La Ti2 Al9 O19 For reflections over 40 ° 2θ CuKα1 was used. Silicon used as an external stand.
PSC: mC248. Mwt: 751.16. Volume[CD]: 2425 76.

2θ	Int	h	k	l	2θ	Int	h	k
7 805*	21	2	0	0	30.256*	6	5	1
8 959*	42	1	1	0	30.387*	5	1	3
13.219*	4	1	1	1	31.405*	999	5	3
14 274*	1	3	1	0	31.405*	999	6	2
16 010*	3	3	1	$\bar{1}$	31 828*	111	7	1
17.951*	2	3	1	1	32.144*	251	2	2
18 457*	4	0	2	1	32.402*	142	6	0
19 591*	75	2	2	$\bar{1}$	32.732*	85	5	1
20.702*	7	2	2	1	33 399*	41	2	4
21.033*	15	2	0	2	33.655*	70	5	3
21.412*	6	5	1	0	33.851*	88	3	3
22.087*	11	5	1	$\bar{1}$	34.063*	28	2	2
22.445*	12	4	0	$\bar{2}$	34.445*	12	8	0
23 512*	38	4	2	$\bar{1}$	35.029*	9	2	4
23 845*	3	6	0	0	35.864*	65	8	2
24 472*	31	1	3	0	36.224*	22	4	4
24.472*	31	0	2	2	36.827*	98	$\bar{9}$	1
24 703*	4	3	1	2	37.218*	38	0	0
25 337*	10	4	2	1	37.775*	214	2	4
26.413*	22	1	3	1	37.775*	214	1	1
26.911*	13	3	3	0	38.285*	4	4	0
27 894*	46	6	0	$\bar{2}$	38 961*	26	1	1
27.894*	46	3	3	$\bar{1}$	39.505*	22	9	1
28.813*	156	1	1	$\bar{3}$	40.202*	25	10	0
29 126*	80	3	3	1	41.312*	78	6	0
29 661*	55	3	1	$\bar{3}$	42.073*	182	4	4

2θ	Int	h	k	l	2θ	Int	h	k	l	2θ	Int	h	k	l
42 963*	128	4	0	4	61.087*	3	8	4	4	91 550*	3	21	1	$\bar{1}$
42 903*	128	6	2	3	64 814*	72	4	2	6	91 550*	3	8	8	4
43 275*	226	6	4	$\bar{2}$	65 529*	150	12	4	2	92 925*	9	12	8	2
44 188*	10	7	3	3	66.661*	196	16	0	0	92 925*	9	19	3	2
44.772*	6	11	1	$\bar{1}$	67.378*	11	7	7	1	93.261*	13	4	6	7
45.005*	4	3	3	$\bar{4}$	67.783*	128	14	4	$\bar{2}$	94.015*	9	19	1	3
45.772*	48	8	0	$\bar{4}$	68.524*	6	10	2	$\bar{6}$	94 422*	13	6	10	1
46.487*	53	6	4	2	68.524*	6	5	1	7	94.752*	12	20	4	$\bar{2}$
47.172*	6	10	0	2	69.385*	5	2	2	7	95 326*	22	10	6	7
47.429*	19	3	1	5	69.776*	4	8	6	3	96.176*	7	2	8	6
47.816*	109	6	0	4	70 482*	7	[0	7	0]	96.877*	6	8	10	1
48.011*	193	3	3	4	70.983*	6	2	8	2	97 217*	18	10	8	4
48 665*	4	10	2	$\bar{3}$	71 210*	8	4	8	1	98 911*	3	4	8	6
49.118*	2	5	1	$\bar{5}$	71.871*	8	3	1	7	100 444	11	6	4	$\bar{9}$
49.844*	13	11	1	$\bar{3}$	72.831*	8	6	8	0	101.176	37	3	11	6
51.142*	16	11	3	0	73 373*	7	14	4	2	102 979	4	2	4	9
51.259*	18	2	6	1	73 874*	5	11	3	$\bar{6}$	103 961	3	20	2	6
51.944*	68	8	4	2	73.874*	5	10	6	$\bar{4}$	104 777	6	3	11	2
52.172*	7	4	6	0	74.271*	8	14	4	$\bar{4}$	105 279	5	16	8	1
53.138*	20	13	1	$\bar{1}$	75 324*	15	4	2	7	105 279	5	21	5	$\bar{2}$
53.807*	31	10	4	$\bar{2}$	75 710*	19	1	8	$\bar{3}$	106 560	4	1	11	3
54.830*	18	4	6	$\bar{2}$	76.174*	6	15	5	$\bar{1}$	107.521	4	13	9	$\bar{4}$
55.259*	18	12	0	2	77.372*	7	11	3	5	107 871	16	20	6	3
56.156*	58	13	1	1	77 597*	11	18	2	$\bar{1}$	108 322	13	15	7	$\bar{6}$
57.152*	80	8	4	$\bar{4}$	78 518*	11	14	6	$\bar{1}$	109 667	7	10	4	8
57.767*	11	14	0	$\bar{2}$	79.925*	5	9	5	5	111 975	10	20	2	7
58 365*	13	10	4	2	80.816*	4	7	7	4	113 679	6	14	4	7
58 508*	20	13	3	$\bar{1}$	81.336*	5	19	1	$\bar{2}$	114 779	6	11	0	6
58.508*	20	5	1	6	81.336*	5	2	0	8	114 779	6	22	4	2
59 418*	11	14	2	1	82 007*	4	19	1	0	117 973	13	18	8	$\bar{4}$
59.418*	11	6	2	5	82 225*	5	13	7	1	117 973	13	21	3	4
60.064*	14	14	2	0	82.514*	6	6	8	$\bar{4}$	119 898	7	8	10	$\bar{6}$
60.064*	14	7	1	5	83.592*	8	4	8	4	120 830	5	24	4	0
60 452*	133	7	5	3	84.830*	2	9	7	5	122 463	27	25	1	1
60.955*	5	3	7	1	85.371*	8	19	3	$\bar{1}$					
60.955*	5	7	5	$\bar{4}$	86 679*	20	20	0	0					
61.315*	23	13	3	1	87.979*	2	2	8	5					
61.473*	36	9	3	$\bar{5}$	88.479*	2	6	8	$\bar{5}$					
61.473*	36	6	2	$\bar{6}$	88.479*	2	9	9	$\bar{1}$					
62.123*	6	1	7	2	89 128*	3								
62.508*	20	5	5	4	89 830*	10	20	2	3					
62 508*	20	5	7	1	90.292*	13	18	2	$\bar{3}$					
63 560*	1	5	7	1	90 909*	4	19	3	$\bar{4}$					

composition.

TABLE: 3.5 X-Ray data for the various phases arranged in ascending '2θ'.

2θ	Intensity	h	k	l	phases
18.785	18	1	0	1	$SrAl_{12}O_{19}$
20.027	30	1	0	2	$SrAl_{12}O_{19}$
22.783	20	1	0	0	$SrTiO_3$
24.164	12	0	0	6	$SrAl_{12}O_{19}$
24.502	6	1	0	4	$SrAl_{12}O_{19}$
25.584	75	0	1	2	Al_2O_3
27.249	4	1	0	5	$SrAl_{12}O_{19}$
31.405	999	5	3	0	$SrTi_3Al_8O_{19}$
31.995	55	1	1	0	$SrAl_{12}O_{19}$
32.411	20	0	0	8	$SrAl_{12}O_{19}$
32.424	100	1	1	0	**$SrTiO_3$**
33.026	16	1	1	2	$SrAl_{12}O_{19}$
33.862	95	1	0	7	$SrAl_{12}O_{19}$
35.136	90	1	0	4	Al_2O_3
36.040	100	1	1	4	$SrAl_{12}O_{19}$
37.120	7	2	0	0	**$SrAl_{12}O_{19}$**
37.441	5	1	0	8	$SrAl_{12}O_{19}$
37.784	5	1	1	0	Al_2O_3
38.100	40	2	0	2	$SrAl_{12}O_{19}$
39.133	40	2	0	3	**$SrAl_{12}O_{19}$**
39.984	30	1	1	1	$SrTiO_3$
40.700	14	2	0	4	**$SrAl_{12}O_{19}$**
40.835	20	0	0	10	**$SrAl_{12}O_{19}$**
41.284	5	1	0	9	**$SrAl_{12}O_{19}$**

41.683	<1	0	0	6	Al_2O_3
42.611	70	2	0	5	**$SrAl_{12}O_{19}$**
43.362	100	1	1	3	**Al_2O_3**
44.785	45	2	0	6	**$SrAl_{12}O_{19}$**
46.183	2	2	0	2	**Al_2O_3**
46.333	2	1	1	8	$SrAl_{12}O_{19}$
46.483	7	2	0	0	$SrTiO_3$
49.126	50	1	0	11	$SrAl_{12}O_{19}$
50.019	3	2	1	1	$SrAl_{12}O_{19}$
50.136	3	2	0	8	**$SrAl_{12}O_{19}$**
51.469	2	2	1	3	$SrAl_{12}O_{19}$
52.357	3	2	1	0	$SrTiO_3$
52.551	45	0	2	4	Al_2O_3
52.780	5	1	1	10	$SrAl_{12}O_{19}$
53.110	11	2	0	9	$SrAl_{12}O_{19}$
56.402	3	2	0	10	$SrAl_{12}O_{19}$
57.012	6	3	0	0	$SrAl_{12}O_{19}$
57.166	5	3	0	1	$SrAl_{12}O_{19}$
57.518	80	1	1	6	Al_2O_3
57.754	4	3	0	2	$SrAl_{12}O_{19}$
57.794	40	2	1	1	**$SrTiO_3$**
58.274	35	2	1	7	$SrAl_{12}O_{19}$
58.477	25	0	0	14	$SrAl_{12}O_{19}$
58.681	5	3	0	3	$SrAl_{12}O_{19}$
59.682	30	3	0	4	$SrAl_{12}O_{19}$
59.767	4	2	1	1	Al_2O_3
59.938	55	2	0	11	$SrAl_{12}O_{19}$
60.197	6	1	1	12	$SrAl_{12}O_{19}$

60.676	4	2	1	8	**$SrAl_{12}O_{19}$**
61.164	6	1	2	2	Al_2O_3
61.344	8	0	1	8	Al_2O_3
63.443	4	2	1	9	**$SrAl_{12}O_{19}$**
66.333	4	2	1	10	$SrAl_{12}O_{19}$
66.547	30	2	1	4	Al_2O_3
66.978	50	2	2	0	$SrAl_{12}O_{19}$
67.141	30	3	0	8	$SrAl_{12}O_{19}$
67.803	25	2	2	0	**$SrTiO_3$**
68.196	50	3	0	0	Al_2O_3
70.357	2	1	2	5	Al_2O_3
71.871	8	3	1	7	$SrTi_3Al_8O_{19}$
72.543	1	3	0	0	$SrTiO_3$
74.266	4	2	0	8	Al_2O_3
76.880	16	1	0	10	Al_2O_3
77.175	15	3	1	0	$SrTiO_3$
77.227	8	1	1	9	Al_2O_3
80.692	8	2	2	0	Al_2O_3

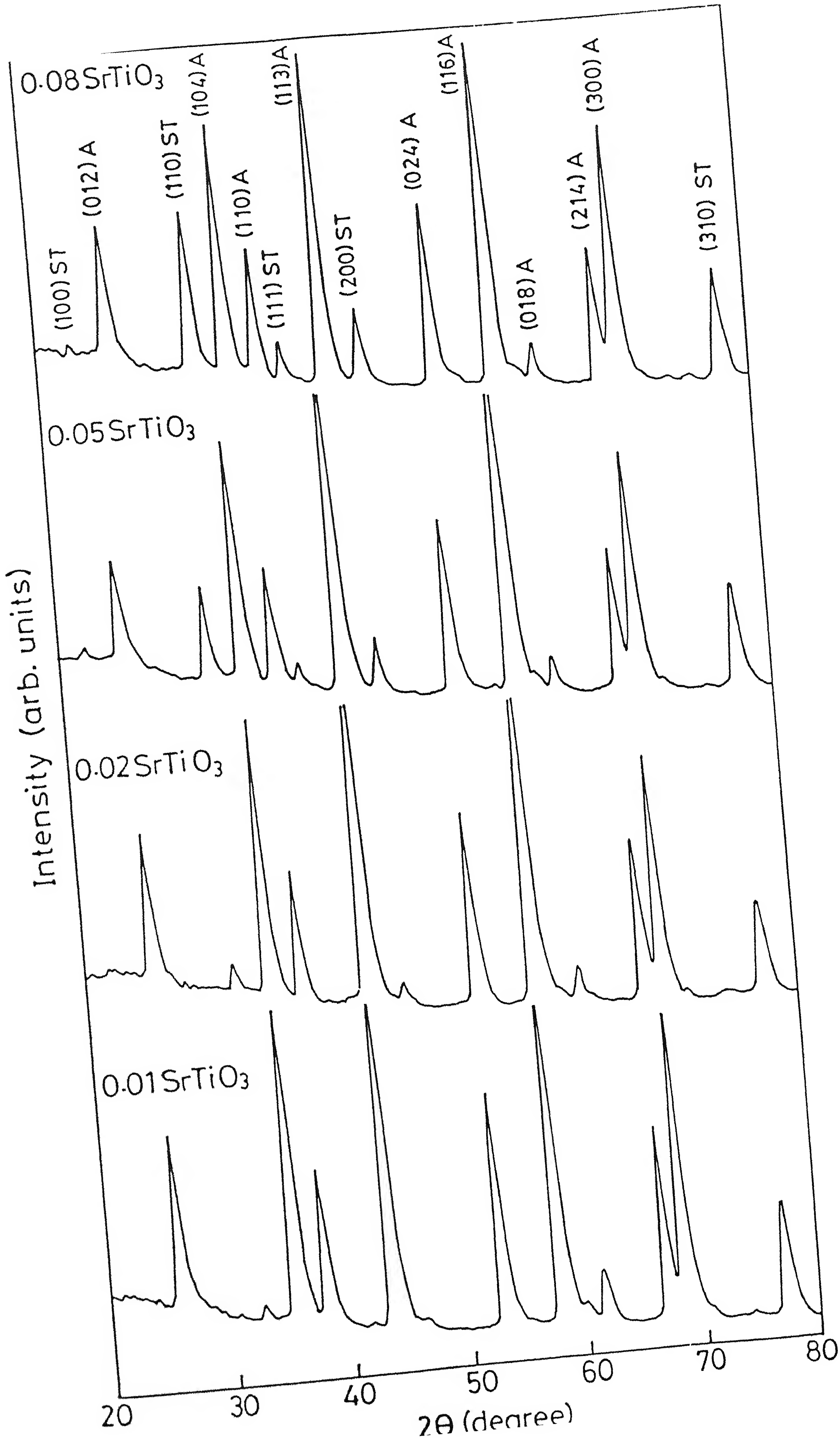

0.08 SrTiO3
(100) ST
(012) A
(110) ST
(104) A
(110) A
(111) ST
(113) A
(200) ST
(024) A
(116) A
(018) A
(214) A
(300) A
(310) ST
0.05 SrTiO3
0.02 SrTiO3
0.01 SrTiO3
Intensity (arb. units)
20
30
40
50
60
70
80
2θ (degree)

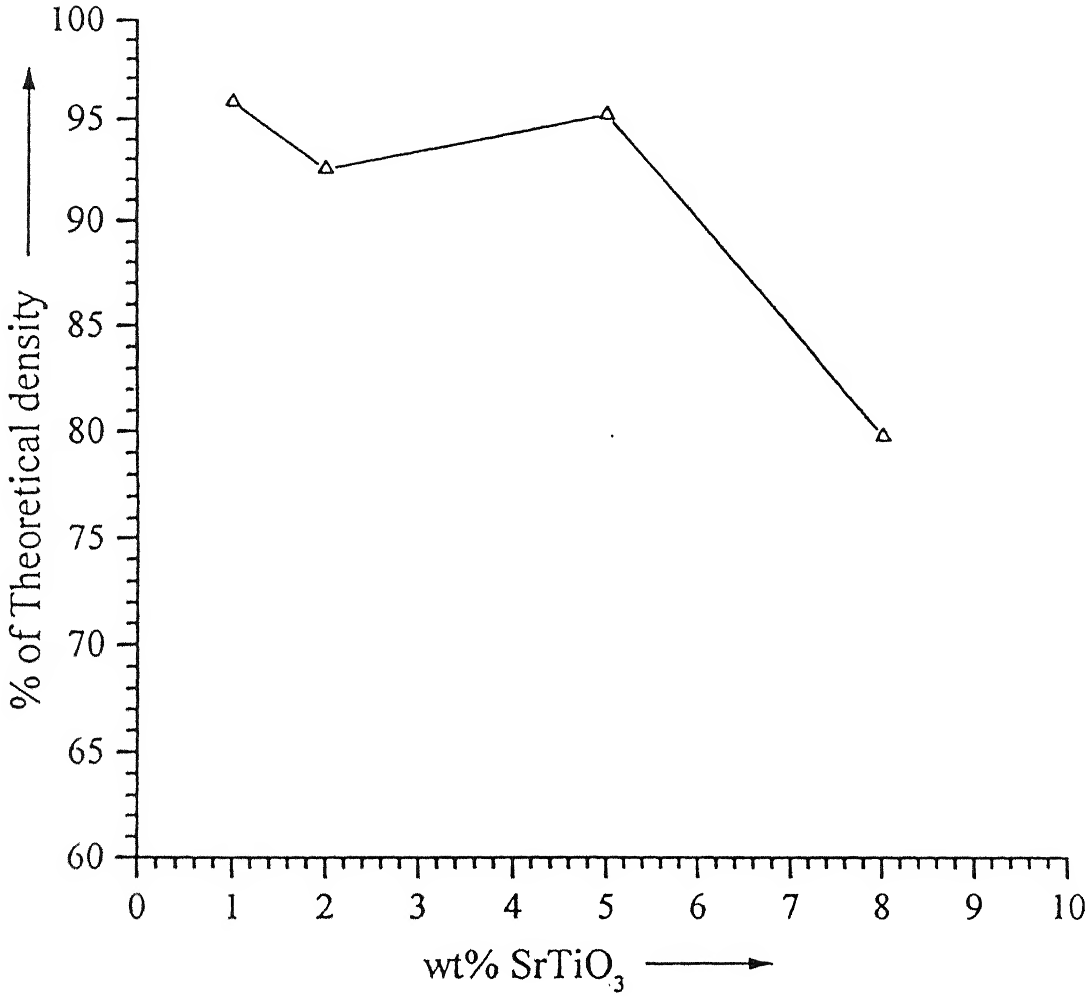

Figure 3.2: Variation of density with weight fraction of $SrTiO_3$.

TABLE: 3.6 Density of pellets from powders calcined at 1100°C for 4 hours and sintered at 1400°C for 2 hours for different compositions.

Nominal Composition wt % $SrTiO_3$	Theoretical Density gm/cm^3.	% Theoretical Density
1	3.996	93.77, 94.04, 93.85, 94.08, 94.95, 95.9
2	4.003	91.84, 92.62, 91.11, 91.75, 90.38, 90.55, 90.25, 90.80
5	4.0317	95.89, 95.96, 96.06, 95.39, 95.45, 94.91, 94.34, 95.27
8	4.06	85.65, 85.25, 84.90, 85.52, 79.96, 79.97

3.3 Phases in the sintered samples

Figure 3.3 shows the XRD patterns of (1-x) Al_2O_3-x$SrTiO_3$ sintered at 1400°c for 2 hours. The various phases present in the sintered samples were determined in the same manner as in the case of calcined powder .The phases obtained are Al_2O_3, $SrTiO_3$, $SrAl_{12}O_{19}$ and $SrTi_3Al_8O_{19}$. The $SrTi_3Al_8O_{19}$ phase is in small amount in the 5% and 8% $SrTiO_3$ samples (peaks at $2\theta = 31.4$ and 71.9) and not detectable at lower composition . As x increases the intensity of the (113) line (100%) for Al_2O_3 decreases in the range of x=0.01 to 0.05 and then increases for x=0.08. The other reflections from Al_2O_3 i.e., (012), (104), (024), and (116) also show the same trend.

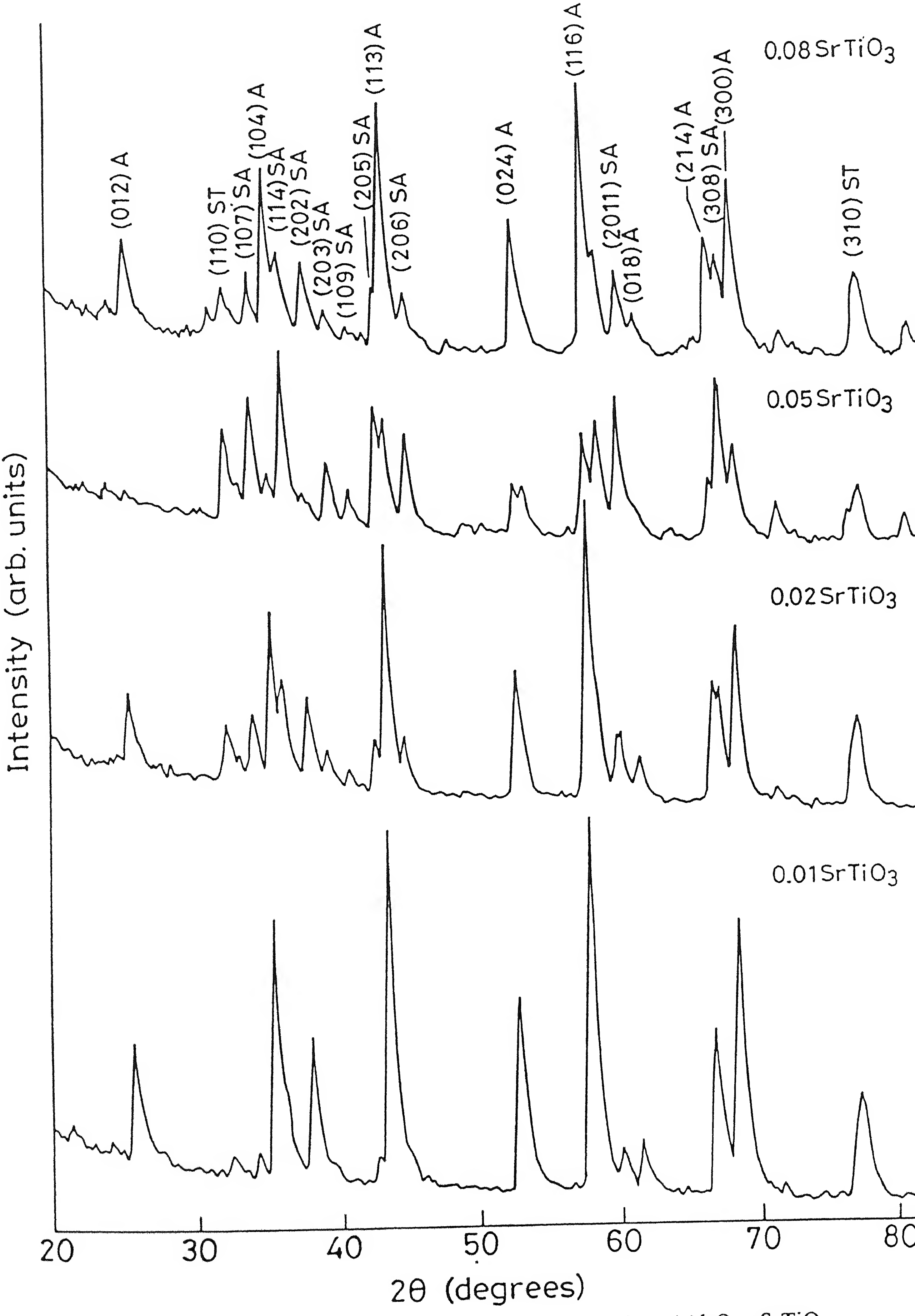

Figure 3.3: X-ray diffractograms for sintered samples of $(1-x)Al_2O_3-xSrTiO_3$.

TABLE: 3.7 Comparision of phases in our samples with phase diagram[14]. The first column is the composition of our samples and the second column is the nearest composition for which data are available.

wt% $SrTiO_3$ in batch	Mole % in batch			Phases from phase diagram	Ratio of 100% peaks in the obtained phases
	Al_2O_3	SrO	TiO_2		.
1	98.89	0.55	0.55	Al_2O_3,$SrAl_{12}O_{19}$,$SrTi_3Al_8O_{19}$	80.5 : 2.4 : 17.1
2	97.76	1.12	1.12	Do	60.5 : 13.1 : 26.4
5	94.46	2.77	2.77	Do	30.4 : 23.2 : 46.4
8	91.18	4.4	4.4	Do	69.6 : 8.7 : 21.7

For $SrAl_{12}O_{19}$ phase the intensity of the 100% (114) line increases from x=0.01 to 0.05 then decreases for x=0.08. The other lines i.e., (107), (205), and (2,0,11) also show this behaviour. For $SrTiO_3$ phase the peak intensity increases for x=0.01 to 0.05 and then decreases for x=0.08 for 100% (110) peak. These trends are reflected in the ratios of the 100% peaks of Al_2O_3, $SrTiO_3$ and $SrAl_{12}O_{19}$ given in table 3.7.

Zandbergan and Ijdo[14] have investigated the phase relationships in the system SrO-TiO_2-Al_2O_3 . The phase diagram for the system at 1300°C is given in figure 3.4(a) .The various phases which are shown in the figure are Sr_2TiO_4, $Sr_3Ti_2O_7$, $SrTiO_3$, $Sr_3Al_2O_6$, $SrAl_2O_4$, $SrAl_4O_7$, $SrAl_{12}O_{19}$, $TiAl_2O_5$. These are all ternary phases. There are also two quaternary phases. These are $SrTi_3Al_8O_{19}$(x) and $Sr_3TiAl_{10}O_{20}$(y) . An enlarged view of the Al_2O_3 rich corner of the above phase diagram is shown in figure 3.4(b). The compositions corresponding to the

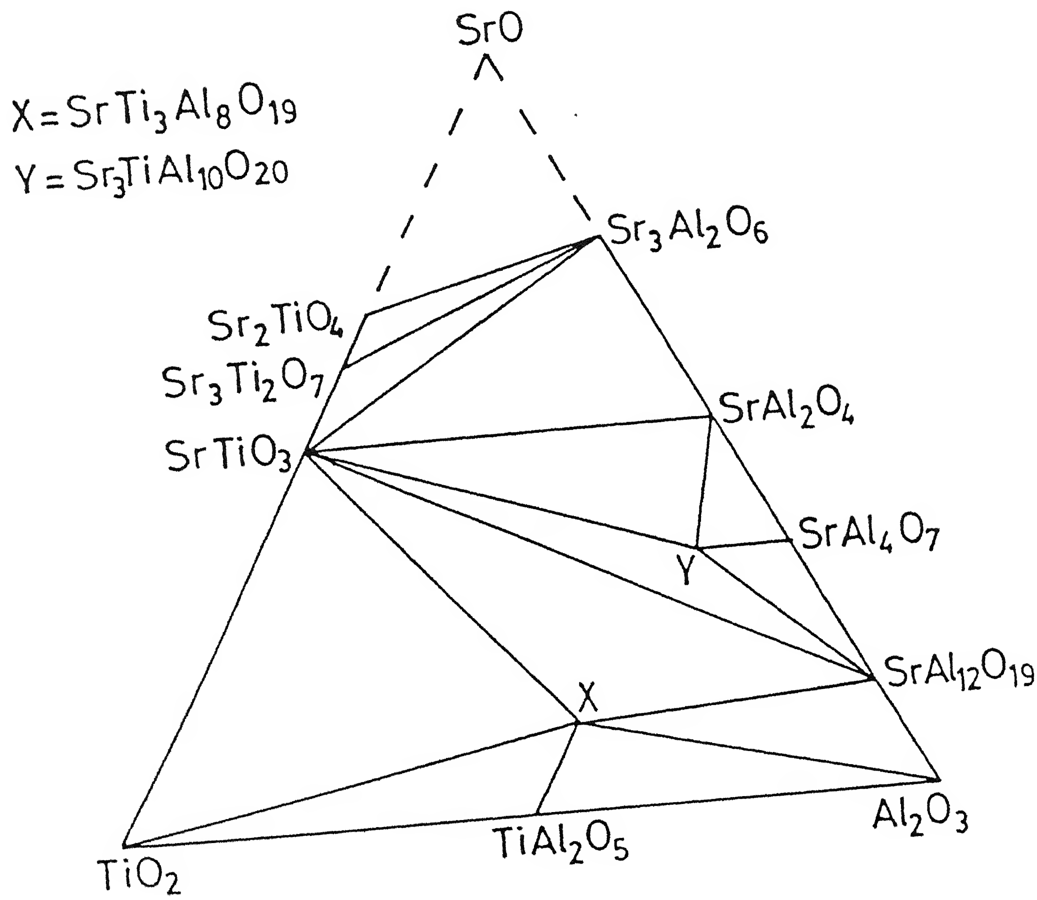

Figure 3.4(a): Phase diagram of the $SrO-TiO_2-Al_2O_3$ system at 1300°C [14].

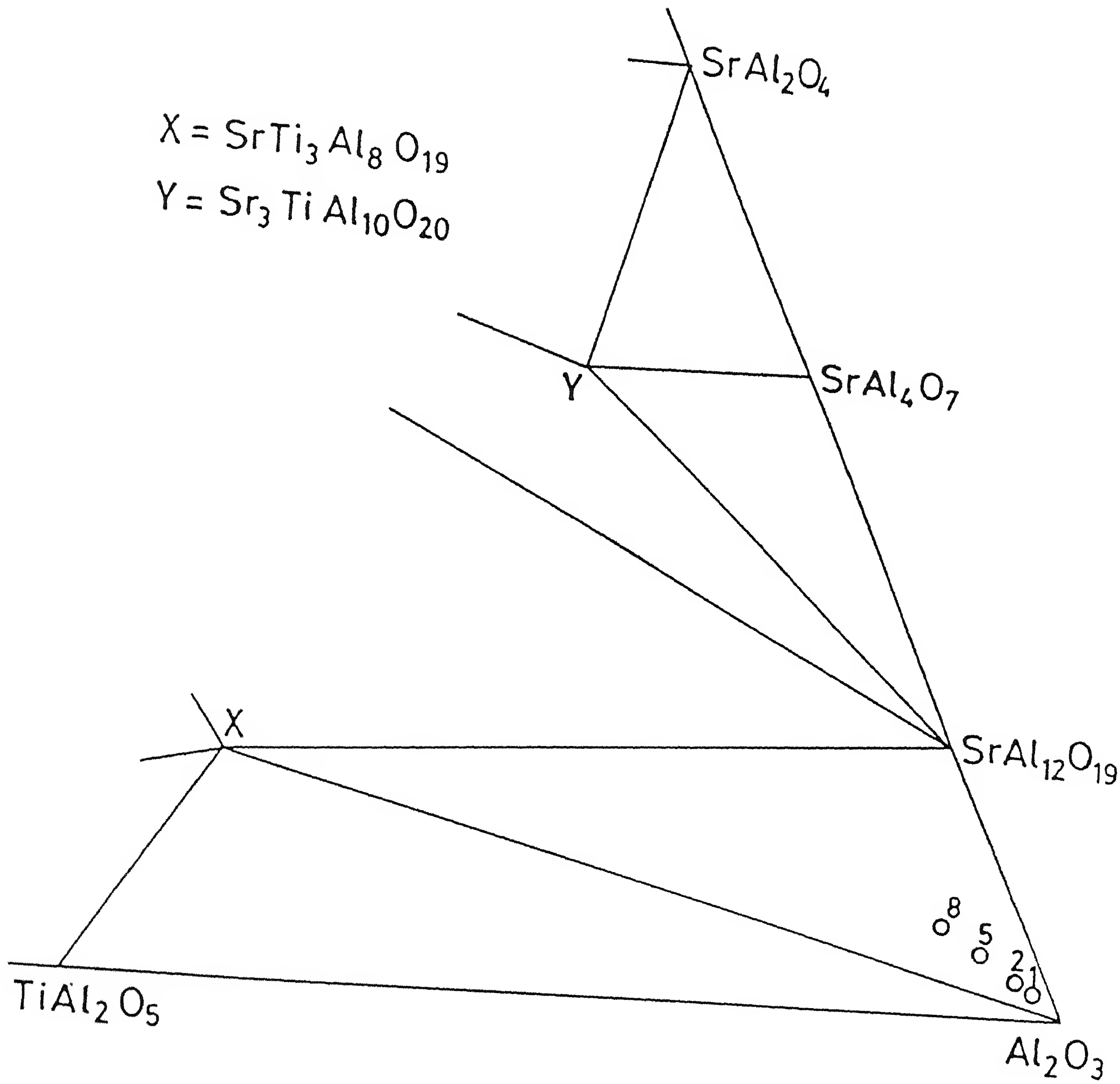

Figure 3.4(b): An enlarged view of the Al_2O_3 rich corner of the phase diagram in the system Al_2O_3-SrO-TiO_2 at 1300°C. Here X= $SrTi_3Al_8O_{19}$, Y= $Sr_3TiAl_{10}O_{20}$ [14].

batch composition are converted to mol % in table 3.7 and marked as 1,2,5,8 in figure 3.4(b). The phases expected for various compositions according to fig 3.4(b) are given in table (3.7). For all compositions according to fig (3.4) the phases should be Al_2O_3, $SrAl_{12}O_{19}$ and $SrTi_3Al_8O_{19}$. But experimentally we get the $SrTiO_3$ phases also in addition to these phases. This is expected because equilibrium is not achieved in our samples in the time used for sintering. Also the phase $SrTi_3Al_8O_{19}$ is found in trace amounts in 5 and 8 wt% compositions.

The variation of lattice parameter with composition gives clear information about solid solution formation. The lattice parameters of rhombohedral Al_2O_3, hexagonal $SrAl_{12}O_{19}$ and cubic $SrTiO_3$ are given in table 3.8, 3.9 and 3.10. These were calculated as described in the experimental seçtion .The lattice parameters of all the three systems are also plotted against the weight fraction of $SrTiO_3$ (fig 3.5-3.9).

TABLE: 3.8 LATTICE PARAMETERS OF Al_2O_3 (Rhombohedral) System.

wt% $SrTiO_3$	a(A^o)	C(A^o)
1	4.7175	12.8314
2	4.7326	12.8592
5	4.7490	12.8722
8	4.7654	13.0663

TABLE: 3.9 LATTICE PARAMETERS OF $SrAl_{12}O_{19}$ (Hexagonal) System

wt% $SrTiO_3$	a(A^o)	c(A^o)
1	5.6615	22.2300
2	5.6529	22.2053
5	5.6009	22.2003
8	5.4871	21.8198

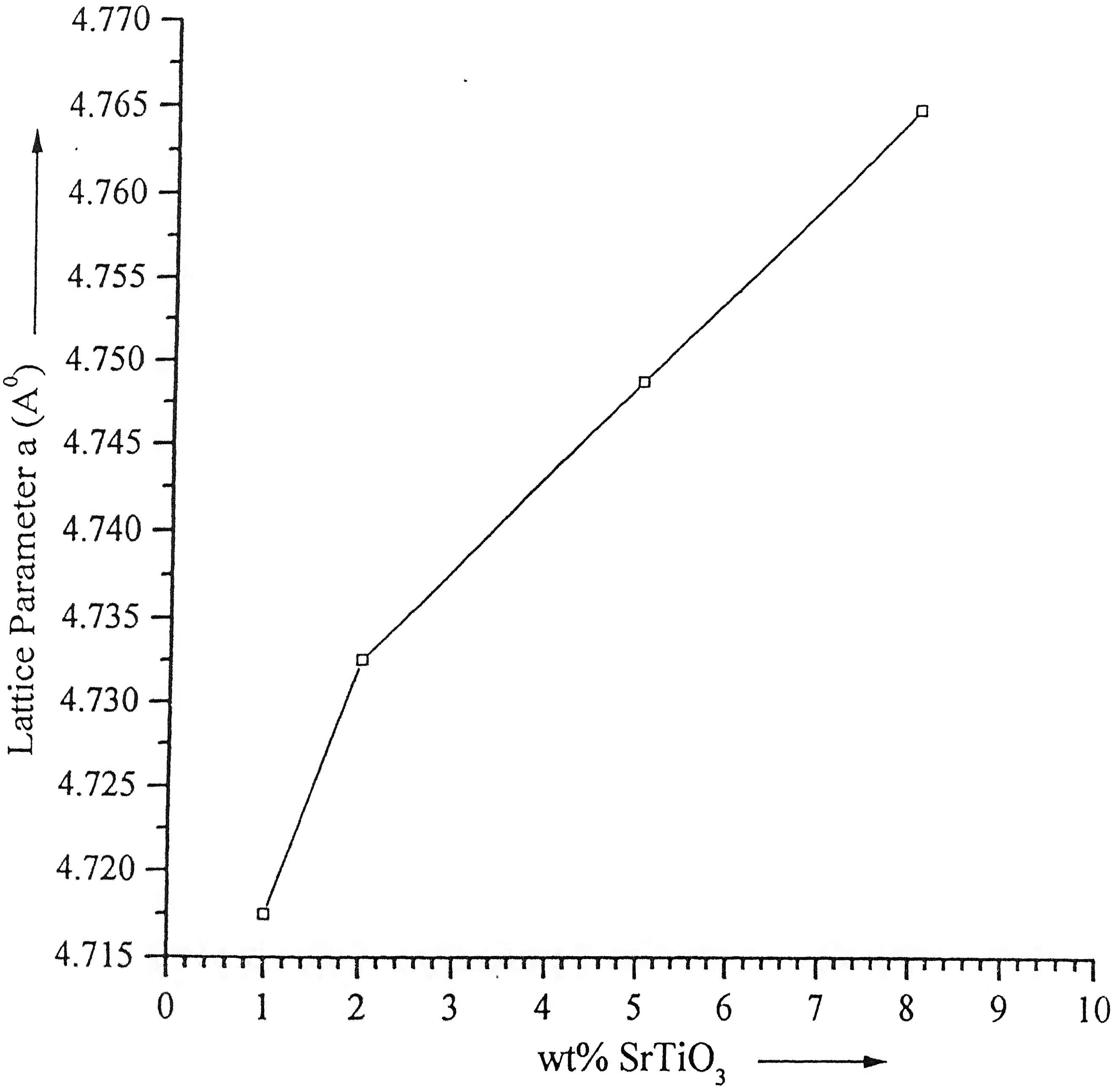

Figure 3.5: Variation of lattice parameter a (Å) of Al_2O_3 with $SrTiO_3$ content.

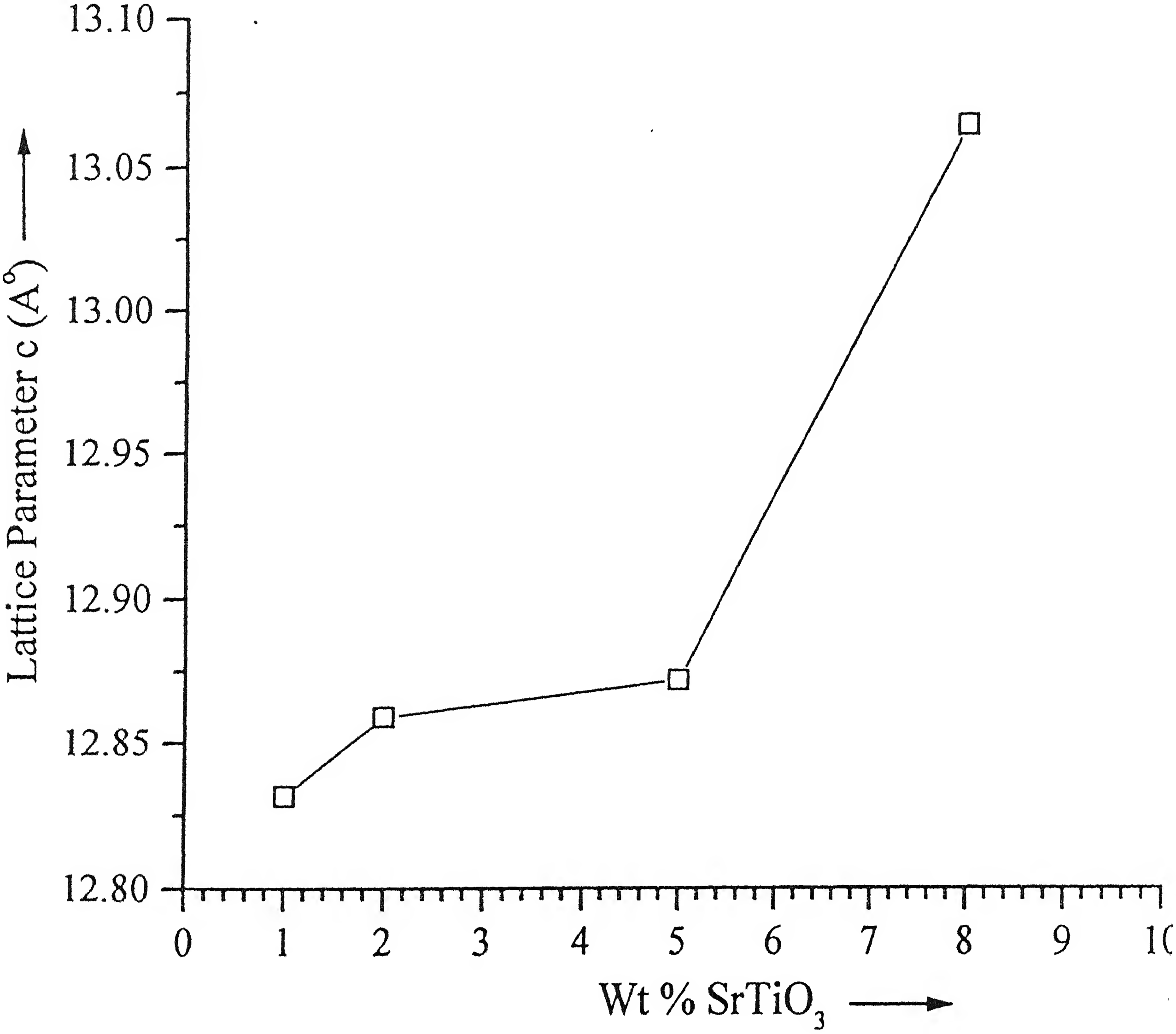

Figure 3.6: Variation of lattice parameter c (Å) of Al_2O_3 with $SrTiO_3$ content.

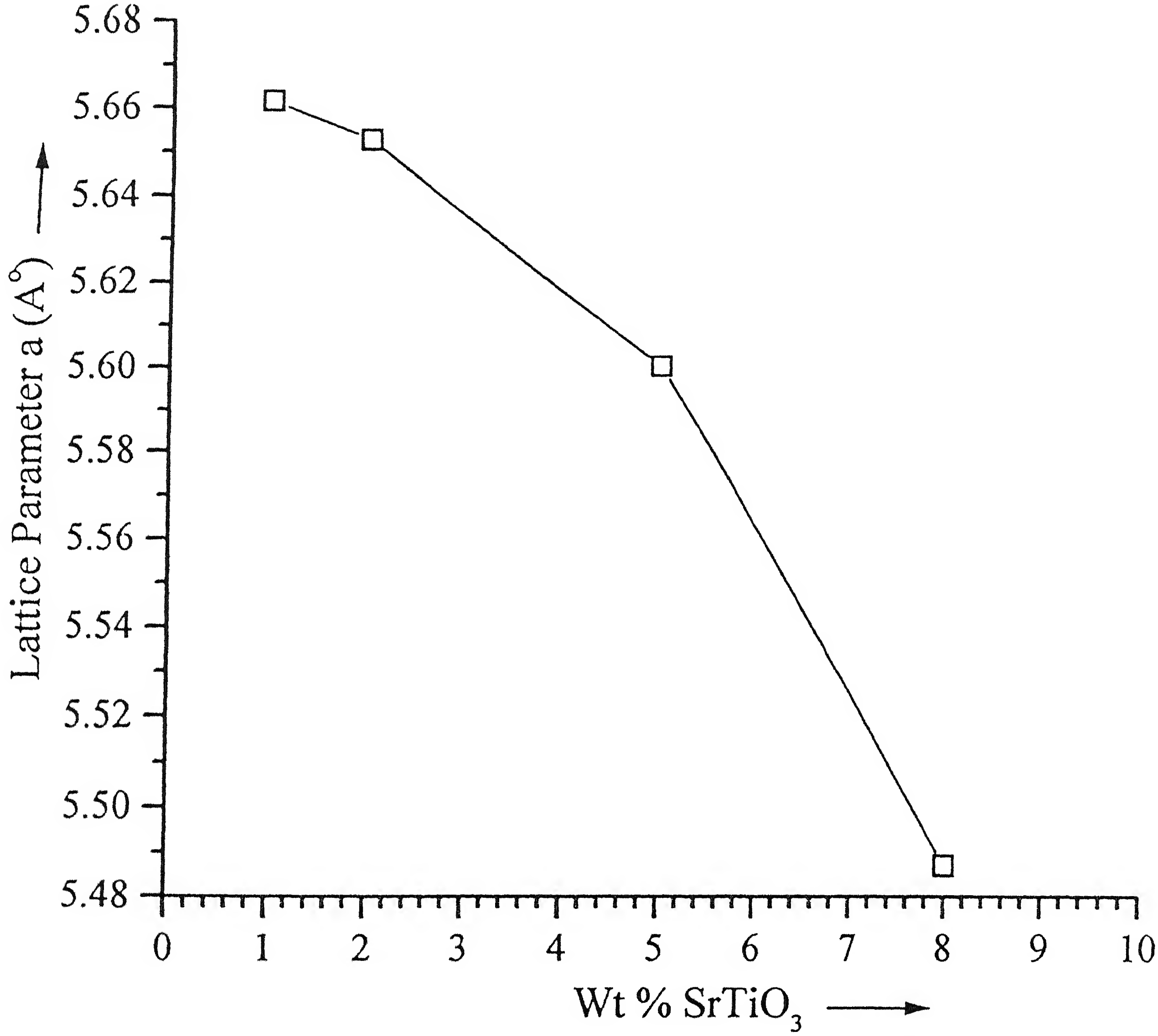

Figure 3.7: Variation of lattice parameter a (Å) of $SrAl_{12}O_{19}$ with $SrTiO_3$ content.

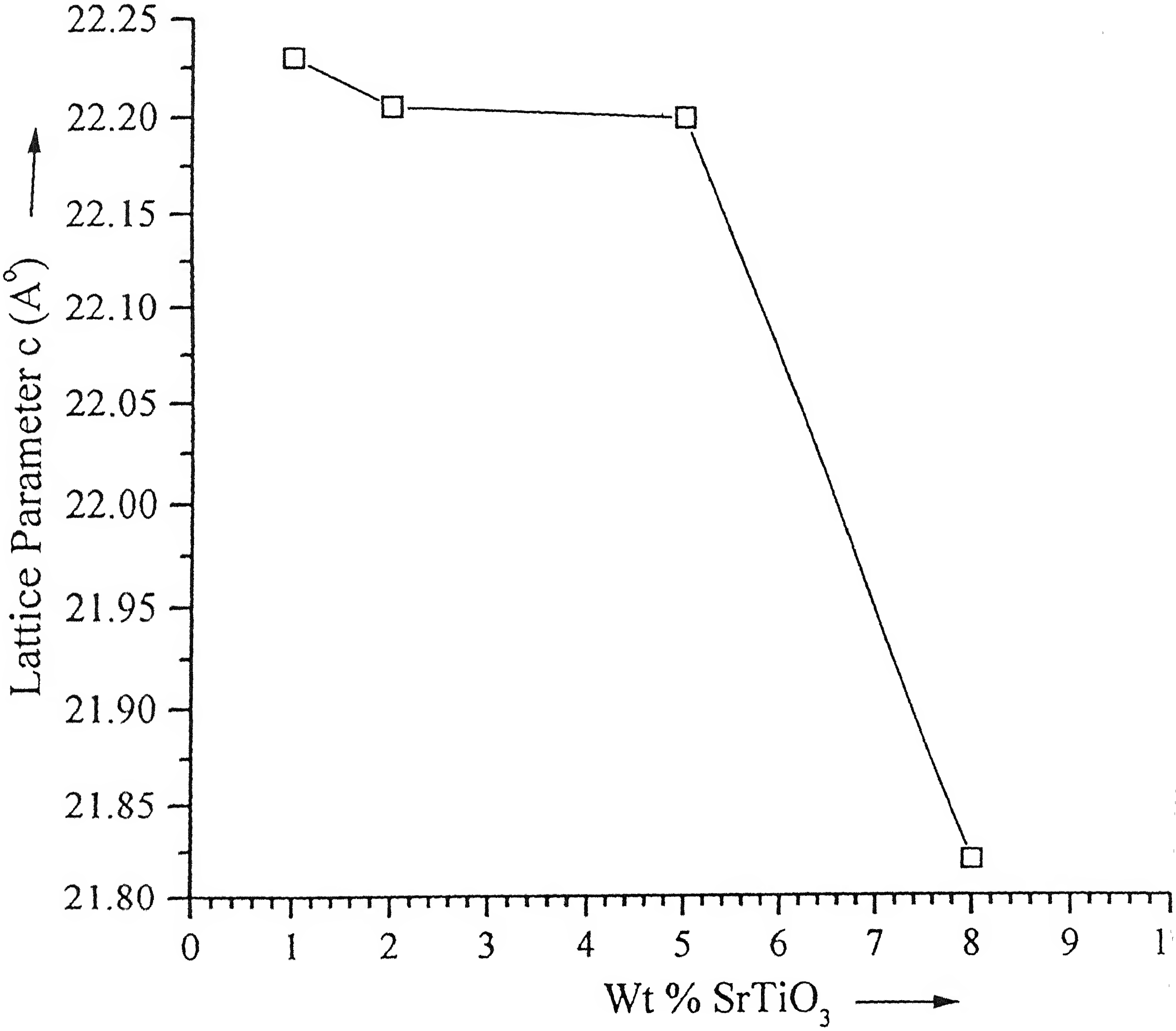

Figure 3.8: Variation of lattice parameter c (Å) of $SrAl_{12}O_{19}$ with $SrTiO_3$ content.

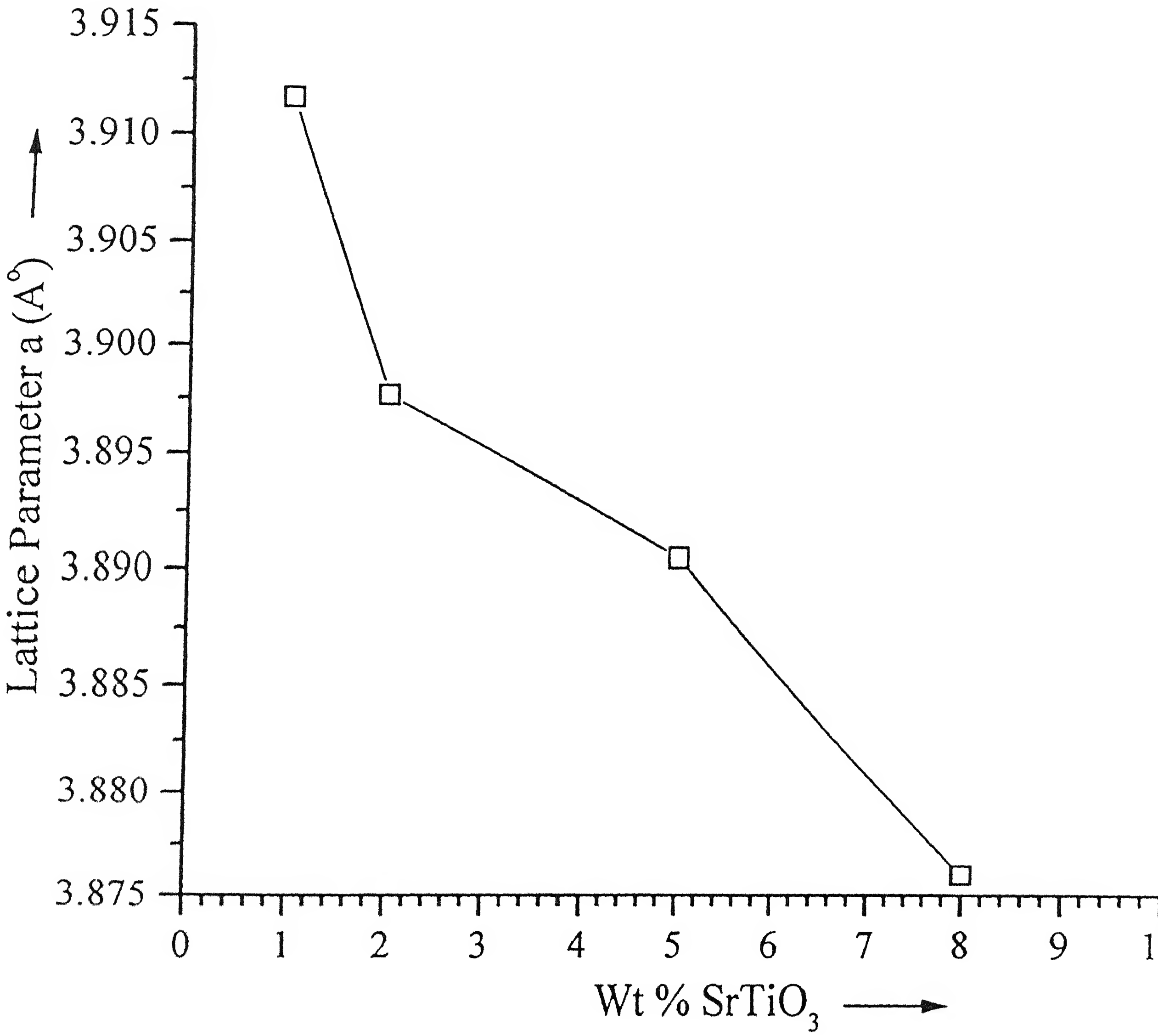

Figure 3.9: Variation of lattice parameter a (Å) of $SrTiO_3$ with $SrTiO_3$ content.

TABLE: 3.10 LATTICE PARAMETER of $SrTiO_3$ (Cubic System)

Wt% $SrTiO_3$	a(A°)
1	3.9117
2	3.8976
5	3.8904
8	3.8760

It is observed that lattice parameters (a, c) of Al_2O_3 system go on increasing as wt % $SrTiO_3$ increases. In case of $SrAl_{12}O_{19}$ system lattice parameter (a, c) decrease as $SrTiO_3$ content increases. For $SrTiO_3$ system also lattice parameter 'a' decreases with increase of $SrTiO_3$ content. The increase of lattice parameter (a, c) with increase of $SrTiO_3$ content in Al_2O_3 system must be due to substitution of Al^{+3}(ionic radius 0.57 A°) ion by the bigger Ti^{+4} (ionic radius 0.64 A°) ion[15]. This may occur according to the following scheme;

$$4Al^{+3} \rightarrow 3Ti^{+4}$$

The changes in the lattice parameter of the $SrAl_{12}O_{19}$ and $SrTiO_3$ phases show that Al^{+3} is also entering their lattices in a reverse substitution.

3.4 Microstructure

The figures 3.10(a) to (e) show the microstructures of the polished surfaces of the samples with different compositions. These SEM micrographs were used to determine the grain size. The grain boundaries of the grains were drawn on a tracing paper. Then keeping the tracing paper on a graph paper, the area enclosed by a grain was determined. This was repeated for a large number of similar grains .The average area of the grain was then calculated. From this the diameter of a circle with equal area was calculated and was taken to be the grain size .The grain

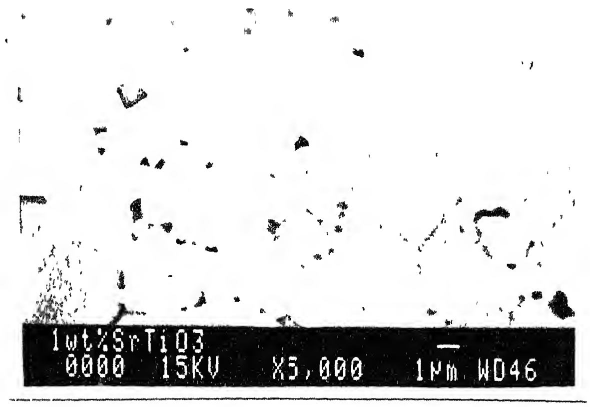
1wt%SrTiO3
0000 15KV X5,000 1μm WD46

(a)

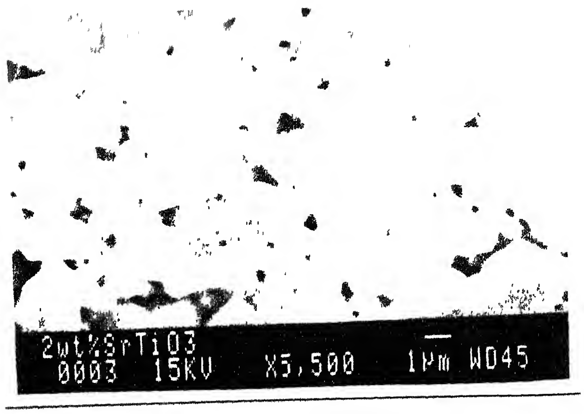
2wt%SrTiO3
0003 15KV X5,500 1μm WD45

(b)

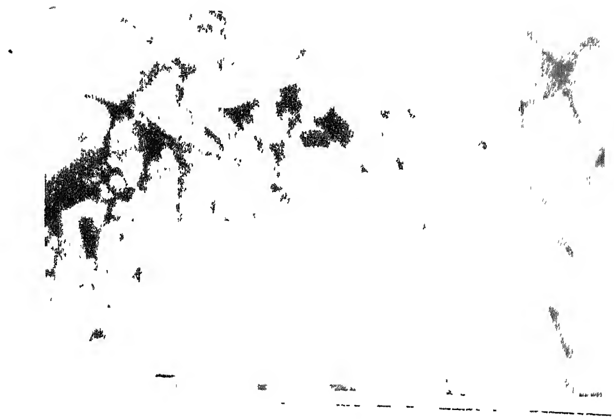

(c)

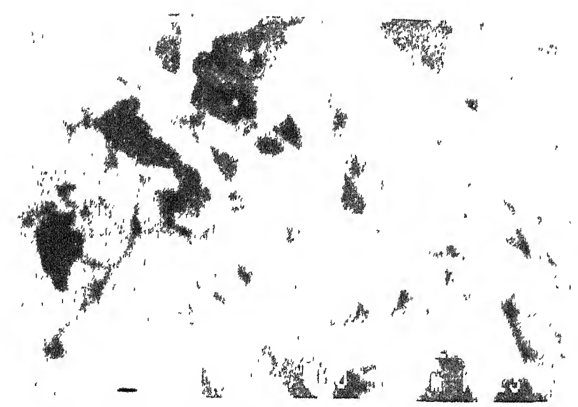

(d)

(e)

Figure 3.10: SEM micrographs of compositions (a) 1wt% $SrTiO_3$ (b) 2 wt% $SrTiO_3$ (c) 5 wt% $SrTiO_3$ (secondary image) (d) 5 wt% $SrTiO_3$ (back scattered image) (e) 8 wt% $SrTiO_3$

size for different types of grains such as (i.e., large, intermediate and small) for all compositions were determined in the same manner. The results are given in table 3.11.

TABLE: 3.11 Grain sizes in different Samples.

	Grain Size (μm)			
wt% $SrTiO_3$	Large grains	Medium Grains	Small grains	% of theoretical density
1	4.6	1.8	1.00	95.9
2	3.0	-----	----	92.62
5	3.8	-----	1.7	95.5
8	2.9	-----	----	80.00

In 1 wt% $SrTiO_3$ samples the grain boundaries are clearly visible. Grain size distribution is trimodal. The bigger grains are of size ~4.6 μm, medium size grains are of 1.8 μm and the finer grains are of size ~1.0 μm. Here the porosity is 4.1%. It appears that the grains of different sizes belong to different phases (Al_2O_3, $SrTiO_3$ and $SrAl_{12}O_{19}$). However this could not be confirmed. In 2 wt% samples the trimodal distribution is not clear, the grains are of average size 3 μm. In 5 wt% $SrTiO_3$ samples, the grain size is bimodal. Also the aspect ratio of most of the grains is considerably larger than 1μm. The bigger grains are of size 3.8 μm and finer grains are of 1.7 μm. For 5 wt% samples we have taken secondary mode images and also back scattered images. From secondary mode images only main phase which is Al_2O_3 phase is detected. But from back scattered images the second phases are also detected along with main phase (Al_2O_3). Here the second phases are $SrTiO_3$ and $SrAl_{12}O_{19}$. In 8 wt % samples the Al_2O_3 grains are of average size 2.9 μm. Thus the grain size generally decreases as the amounts of the phases other

than Al_2O_3 increases. This is expected because the additional phases inhibit the grain growth of the matrix phase (Al_2O_3).

3.5 Dielectric Constant

The variation of dielectric constant with wt% $SrTiO_3$ in the batch is given in fig 3.12. From the figure it is observed that this dielectric constant is 10.52 for x=0.01 and slightly less for the other compositions.

TABLE: 3.12 Dielectric constant (ε_r) of the samples calcined at 1100^{O} c /4hrs and sintered at 1400^{0} C/2hrs.

wt% $SrTiO_3$ in batch	Density gm cm^{3}	ε_r (meas)	ε_r (cal)	ε_r (cal) taking porosity	ε_r of $SrAl_{12}O_{19}$ (cal)	ε_r (cal) using ε_r of $SrAl_{12}O_{19}$ as 3.67
1	95.9	10.52	10.238	9.307	15.9	8.29
2	92.62	9.5	10.48	8.8	3.58	9.55
5	95.45	9.91	11.25	10.08	2.25	11.26
8	79.97	9.45	12.11	7.35	30.9	6.54

The values of the dielectric constant in a multiphase ceramic can be predicted by using a mixture rule. The logarithmic mixture rule ($\log\varepsilon = v_1\log\varepsilon_1 + v_2\log\varepsilon_2$) [16] is usually found to have good agreement with the experimental values. Initial calculation was carried out assuming that only the Al_2O_3 and $SrTiO_3$ phases are present.

For calculation the dielectric constant of Al_2O_3 and $SrTiO_3$ have been taken to be 10 and 205 respectively [10]. The logarithmic mixture rule is used for calculating dielectric constant for 100% dense samples. The results are given in

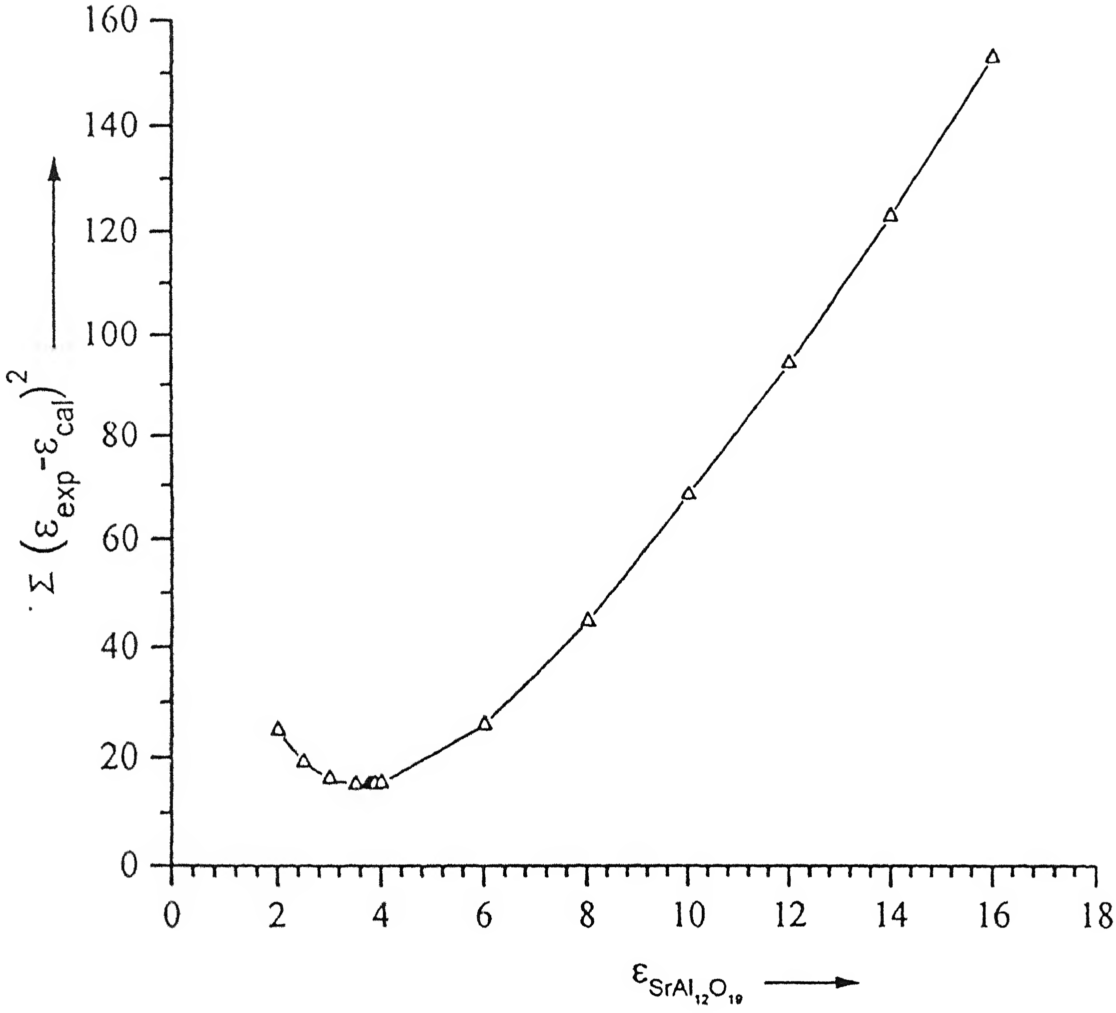

Figure 3.11: Variation of $\varepsilon_{SrAl12O19}$ with $\sum(\varepsilon_{exp}-\varepsilon_{cal})^2$.

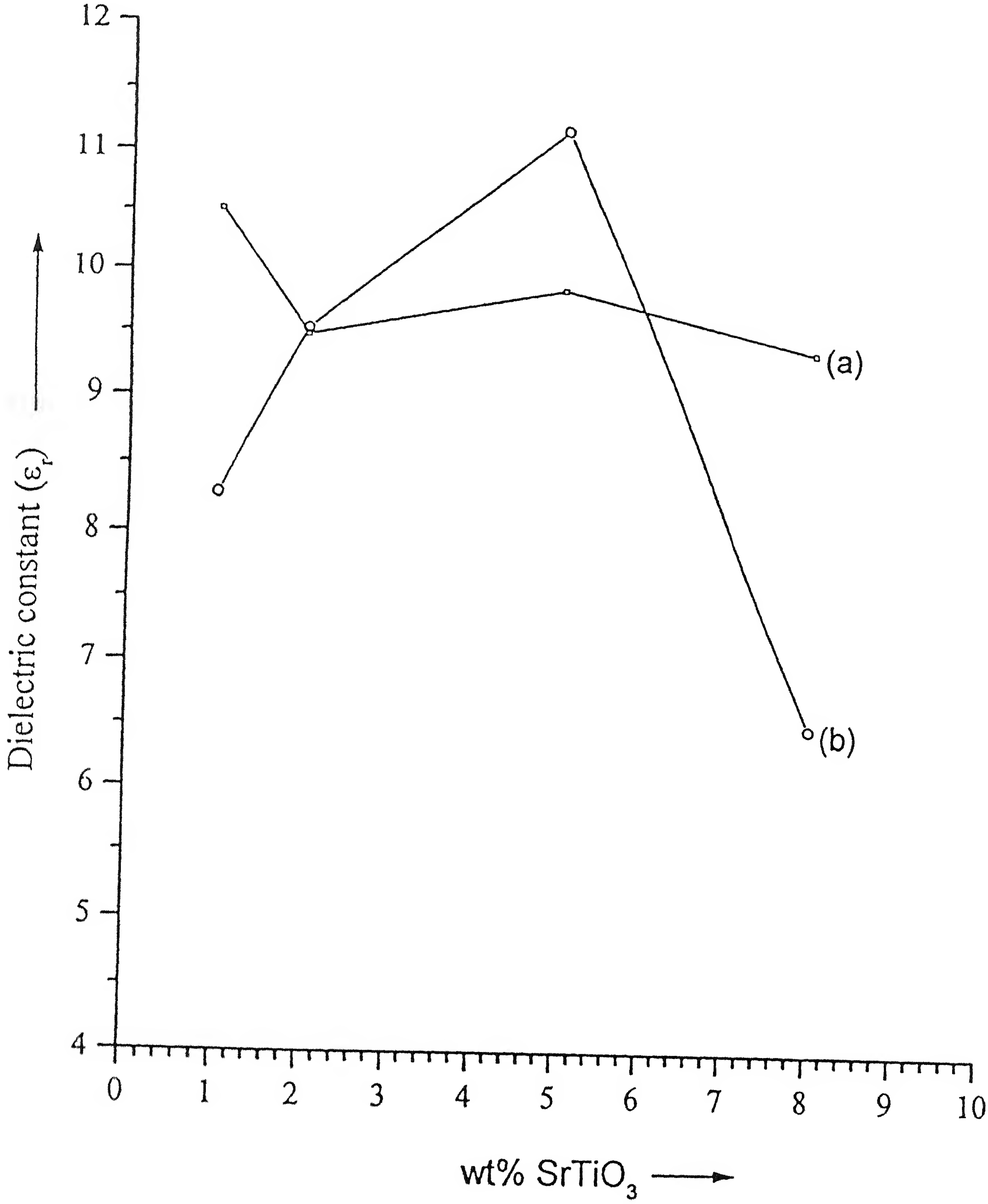

Figure 3.12: Variation of dielectric constant with wt% $SrTiO_3$ (a) measured value (b) calculated value.

table 3.12. The calculated values are next corrected for porosity of the samples. These are also given in table 3.12.

The agreement between the measured and calculated values is not expected to be good as additional phase, mostly $SrAl_{12}O_{19}$ is also present .The dielectric constant of this phase is unknown. However knowing the amount of the three phases from the X-ray data and porosity, as given in table 3.7, and using the measured values of the dielectric constant of the samples, the dielectric constant of the $SrAl_{12}O_{19}$ phase can be calculated. These are also given in table 3.12 .As can be seen, this varies between 2.2 and 30.9. To get a better estimate, different values of dielectric constant of $SrAl_{12}O_{19}$ phase between these two limits were used and the difference between the calculated and measured values of the samples was minimized using the least squares Fig 3.11. The corresponding values of the dielectric constant of $SrAl_{12}O_{19}$ corresponding to the minimum deviation comes out to be 3.67. Using this value of $\varepsilon_{SrAl12O19}$, the dielectric constant for the samples are recalculated taking porosity into account and are tabulated in table 3.12 and plotted in figure 3.12. It is seen that the calculated values agree reasonably with the measured values. A sample calculation is given in Appendix C.

3.6 Temperature Co-efficient of Resonant Frequency (TCF)

The temperature co-efficient of resonant frequency (TCF) data from table 3.13 is plotted against wt% $SrTiO_3$ in fig (3.14). It is observed that TCF increases with the increase of wt% $SrTiO_3$. By taking the TCF of Al_2O_3 and $SrTiO_3$ to be – 67 and +1700 [3], the TCF value of the samples can be calculated assuming that only the two phases (Al_2O_3 and $SrTiO_3$) are present in the nominal amounts and using the relation $TCF = \sum_i V_i\,(TCF)_i$. These values are also plotted in fig 3.14

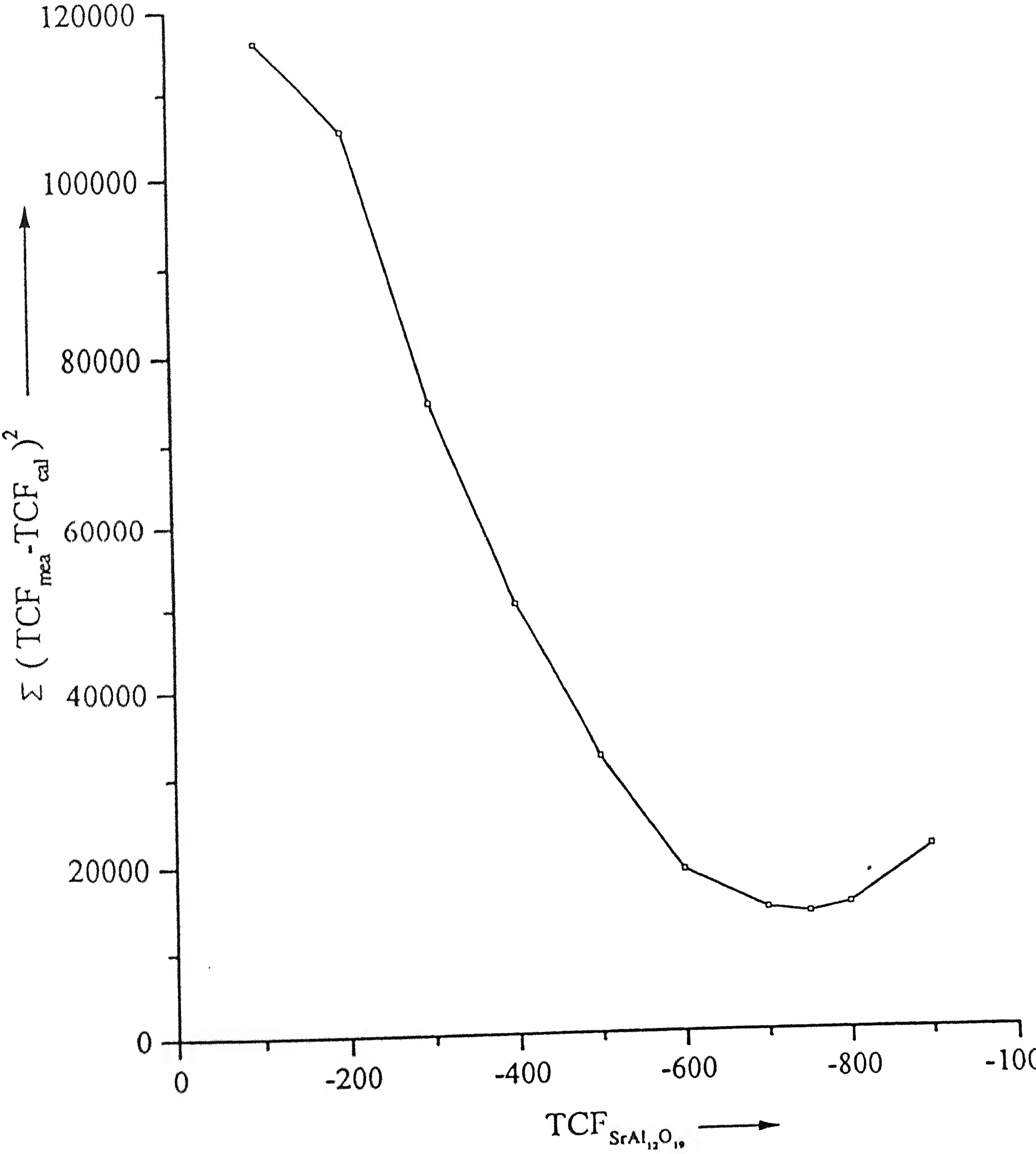

Figure 3.13: Variation of the $TCF_{SrAl12O19}$ with $\Sigma\,(TCF_{mea}-TCF_{cal})^2$.

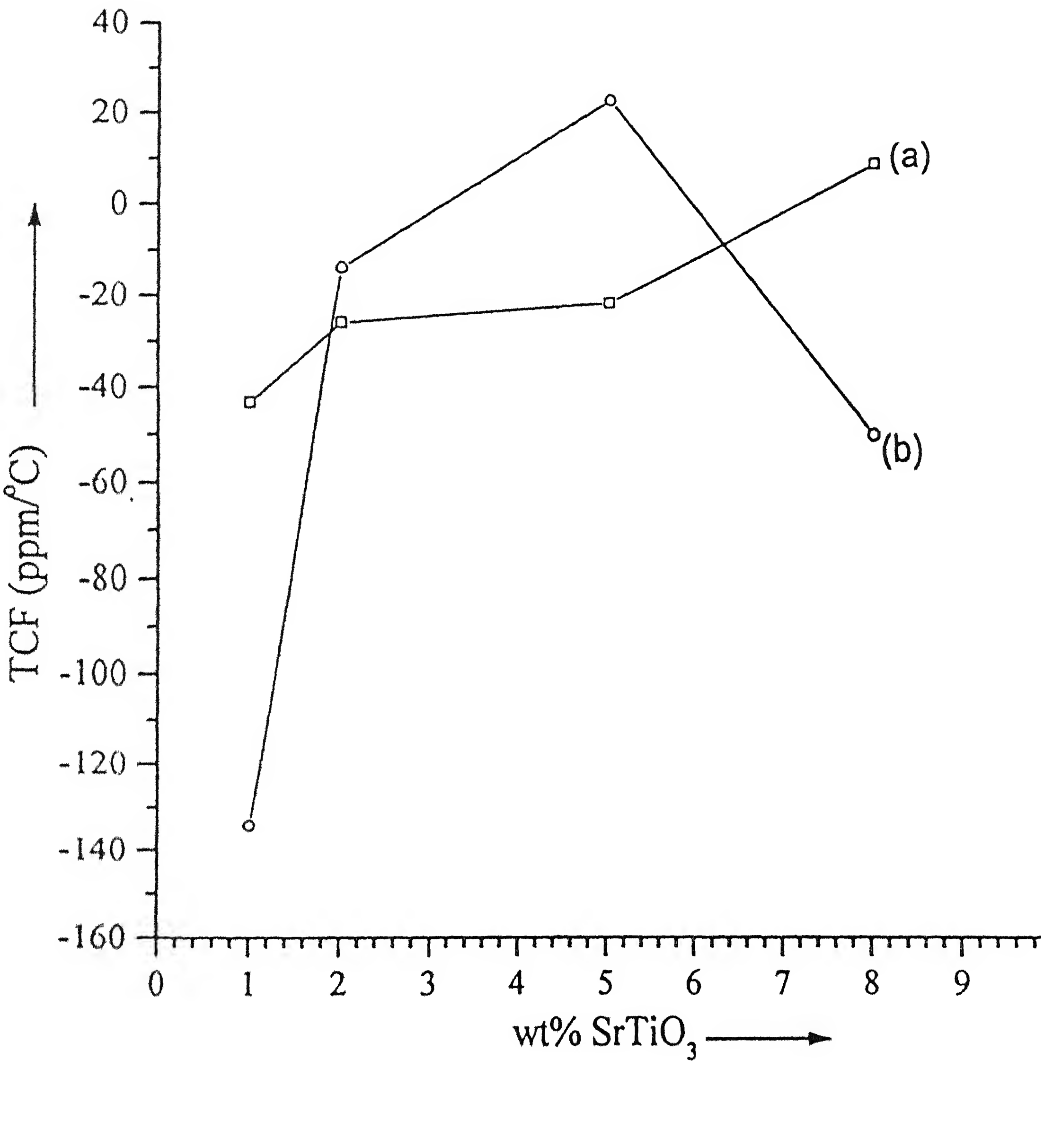

Figure 3.14: Variation of TCF with wt% $SrTiO_3$ (a) measured value (b) calculate value.

TABLE: 3.13 Temperature co-efficient of resonant frequency (TCF) of the samples calcined at 1100^{0}C/4hrs and sintered at 1400^o/2hrs .

wt % $SrTiO_3$	Density	TCF (meas)	TCF (cal)	TCF (cal) Taking porosity	TCF of $SrAl_{12}O_{19}$ (ppm/^{o}c)	TCF(cal) taking ε_r of $SrAl_{12}O_{19}$
1	95.9	-43.0	-53.21	-51	-188.67	-134.1
2	92.62	-25.4	-39.258	-36.36	-800	-13.24
5	95.45	-20.3	2.449	2.337	-851.6	24.65
8	79.97	11.3	45.20	36.146	-403.5	-48.53

Next taking porosity into consideration the TCF value is recalculated and is given in table 3.13. It is observed that there is significance difference between the calculated and the measured values. As wt% $SrTiO_3$ increases, the difference between the measured and the calculated values increases. This poor agreement is expected as the presence of the $SrAl_{12}O_{19}$ phase has not been taken into account. Taking the relative amounts of the three phases (Al_2O_3, $SrAl_{12}O_{19}$ and $SrTiO_3$) from the x-ray peak ratios and porosity the TCF for $SrAl_{12}O_{19}$ phase can be calculated. These values are given in table 3.13. A best estimate of the TCF of $SrAl_{12}O_{19}$ is obtained by the same procedure as described for the dielectric constant. This value of TCF of $SrAl_{12}O_{19}$ is –750 ppm/°C. Using this value, the TCF of the samples are recalculated and plotted in figure 3.14. The agreement is not very good. This may be because the quantitative determination of the phases is not very accurate. However, this calculation does give an idea of the expected value of the TCF of $SrAl_{12}O_{19}$.A sample calculation is given in Appendix D .

3.7 Properties of the co-axial resonators

The dimension and the densities of all the co-axial resonator devices made are given in table 3.14. It is seen that the density decreases as the amount of $SrTiO_3$ increases. Reasonable density of about 95 % is obtained only for th 1 % composition .It may be necessary to improve the processing or to use isostatic pressing to get higher density.

The Q at 1.8 GHz and f_o of 1 wt% $SrTiO_3$ samples are given in table 3.15. A quality factor of ~ 800 is obtained which is acceptable for these devices. The resonant frequency depends on the dimension and can be adjusted depending on the requirements.

The Q and f_o of the other samples could not be measured as the network analyzer started malfunctioning.

TaBLE: 3.14 The dimensions and the densities of all the co-axial resonator devices.

wt% $SrTiO_3$	Sample No	Length	Breath	Height	Dia of Hole	Density	% of (Theo) density
1	3	12.13	12.08	13.1	3.6	3.789	94.82
	4	12.13	12.1	13.18	3.5	3.7613	94.12
2	5	12.94	12.87	13.33	3.8	3.3349	83.27
	6	12.9	12.88	13.34	3.8	3.3404	83.4
5	1	13.1	12.97	13.8	3.8	3.0897	76.6[illegible]
	2	13.05	13.16	13.8	3.7	3.0482	75.6
8	7	13.03	13.12	14.3	3.8	2.9977	73.85
	8	13.0	13.08	14.24	3.7	3.0085	74.11

SUMMARY

In this work ceramics in the system Al_2O_3 –$SrTiO_3$ have been studied with a view to their suitability for application in dielectric resonators .The compositions with weight fraction of $SrTiO_3$, 0.01, 0.02, 0.03 and 0.08 have been studied. It is found that highest density (95 to 96 %) is obtained for composition 5 wt% $SrTiO_3$ followed by the composition 1 wt% $SrTiO_3$. The density obtained for 2 wt% $SrTiO_3$ samples is lower, which is surprising. The 8 wt% $SrTiO_3$ samples sinter poorly to about 85% density. The major phases in the sintered samples are Al_2O_3, $SrTiO_3$ and $SrAl_{12}O_{19}$. The $SrTi_3Al_8O_{19}$ phase is present in small amount in the 5% and 8 % samples. The increase in lattice parameter (a, c) of Al_2O_3 with $SrTiO_3$ content is due to substitution of Al^{+3} ion by bigger Ti^{+4} ion.

The dielectric constant of the samples lies between 9.5 and 10.5. Then attempt was made to estimate the dielectric constant of the phase $SrAl_{12}O_{19}$ by using a logarithmic rule of mixture. The value of the dielectric constant of $SrAl_{12}O_{19}$ thus estimated comes out to be 3.7. However, as the quantities of the various phases were not determined very accurately. This value of 3.7 is only very crude estimate.

The TCF of 1 wt% samples is –43, it changes to –20 for 5 wt% samples and to 11.3 for the 8 wt% samples. Thus it appears possible to obtain a near zero value of the TCF by selecting a composition between 5 and 8 wt%.

Similar to estimation of the dielectric constant, the TCF of the $SrAl_{12}O_{19}$ phase was also estimated using a rule of mixture. This came out to be –750 ppm/°C. Again this is a crude estimate in view of the uncertainity in the amount of phases.

The aim of the investigation was to develop ceramics with dielectric constant of 10 and TCF of about zero. Based on the work done here. It can be said that a

composition containing Al_2O_3-5 to 8 wt% $SrTiO_3$ should yield these properties. However the densities obtained for these compositions are rather low and we need to be further improved by techniques such as cold isostatic pressing.

Co-axial resonator devices prepared using the 1 wt% composition have a quality factor of 800 at 1.8 GHz. This value of 'Q' is in the acceptable range for Co-axial resonator devices.

REFERENCES

[1] Makoto Mizuta, Koji uenoyama, Hitoshi ohsato , Susumu Nishigaki1 and Takashi okuda; " Formation of Tungsten Bronze –Type (Ba $_{6-3x}$Sm $_{8+2x}$)$_{\alpha}$Ti$_{18-x}$Al$_x$O$_{54}$(α 1 · y 36) solid solutions and microwave dielectric properties "; Jpn.J.Appl.Phys.Vol.35(1996)pp.5065-5068 .

[2] G.Lutteke and D.Hennings; " Dielectric resonators for microwave integrated oscillators," philips Tech.Rev.43 pp.35-46 (1986).

[3] Hitoshi ohsato, Atsushi komura , Yuji takag,Susumu Nishigaki and Takashi okuda; " Microwave dielectric properties and sintering of $Ba_{6-3x}R_{8+2x}Ti_{18}O_{54}$ (R Sm,x 2 3) solid solution with added rutile"; Jpn.J.Appl.Phys.Vol.37(1998) pp.5357-5359 .

[4] R.Freer; " Microwave dielectric ceramics an overview", Silic . Ind , 58[9-10] pp191-197 (1993) .

[5] R.W.P King , S .Prasad ; "Fundamental electromagnetic theory and application", Prentice Hall ,Inc. Englewood cliffs ,N.J. pp-500 (1986) .

[6] W.Wersing ; "High frequency ceramic dielectrics and their application for microwave components," Electronic ceramics, edited by B.C.H Steel, Elsevier Applied Science .London, 67-119(1991) .

[7] J.M.Herbert; " Ceramic dielectrics and capacitors," Gorden and Breach Science publishers ,Philadelphia ,pp.124-126 (1992) .

[8] Jen-Yan Hsu, Nan-Chung Wu and Shu-Cheng Yu; " Characterisation of material for low-temperature sintered multilayer ceramic substrates," J.Am.Ceram.Soc, Vol.72[10]pp.1861-1867(1989).

[9] B.Schwartz, " Ceramic Packaging of integrated circuits ," Electronic Ceramics, edited by L.M.Levinson, Marcel Dekker ,Inc , New york , p-28(1987) .

[10] Pai-hsuan sun, Tetsuro nakamura, Yue Jin shan, Yoshiyuki inagumai, Mitsuru itoh and Toshiki kitamura; "Dielectric behaviour of (1-x)$LaAlO_3$-x$SrTiO_3$ solid solution system at microwave frequencies"; Jpn.J.Appl.Phys Vol.37(1998)pp.5625-5629.

[11] G.S.Perry and J.R.Alderton ; "Dielectric properties of Titanate-Alumina ceramics" J.Am .ceram.Soc .vol52[6] pp-348 .

[12] Rasmi Ranjan Das .M.tech thesis submitted to dept. of materials science programme, IIT-Kanpur, November 1998.

[13] B.D.Cullity; " Elements of X-ray diffraction", Addision-Wesley publishing company , Inc p-324-333 (1967) .

[14] H.W.Zandbergen and D.J.W.Ijdo; " New compounds in the system SrO-TiO_2-Al_2O_3 at 1300°c",Materials Res.Bull.Vol.18, pp.371-374(1983) .

[15] Jong H.moon, Hyun S. park, kyung T. lee.Ju H. choi. Dong H. yeo: "Microwave dielectric properties of the (1-x)$La_{2/3}TiO_3$-x$LaAlO_3$ System", Jpn.J.Appl.Phys.Vol.36, (1997)pp.6814-6817 .

[16] W. D. Kingery, "Introduction to Ceramics", by John Wiley and Sons, Inc., pp.686-761 (1960) .

Appendix-A

Weight calculation for a batch .

The general formulae used for a batch preparation is $(1-x)Al_2O_3$-x $SrTiO_3$ .Here 'x' is in weight fraction .

For a w gm batch with composition x wt% $SrTiO_3$.

$$\text{Weight of } SrTiO_3 = \frac{w \times x}{100} \text{ gms}$$

$$\text{Weight of } Al_2O_3 = \frac{w(100-x)}{100}$$

Now the reaction is ,

$$SrCO_3 + TiO_2 \rightarrow SrTiO_3 + CO_2$$

Now 1 mole of $SrTiO_3$ =1 mole of $SrCO_3$

183.5 gms of $SrTiO_3$ = 147.62 gms of $SrCO_3$

$$\frac{wx}{100} \text{ gms of } SrTiO_3 = \frac{147.62}{183.5} \times \frac{wx}{100} \text{ gms of } SrCO_3$$

183.5 gms of $SrTiO_3$ = 79.88 gms of TiO_2

$$\frac{Wx}{100} \text{ gms of } SrTiO_3 = \frac{79.88}{183.5} \times \frac{Wx}{100} \text{ gms of } TiO_2$$

So for a batch of W gms with x wt% $SrTiO_3$ composition ,

$$Al_2O_3 \text{ required} = \frac{w(100-x)}{100} \text{ gms}$$

$$SrCO_3 \text{ required} \quad \frac{147.62}{183.5} \times \frac{Wx}{100} \text{ gms}$$

$$TiO_2 \text{ required} \quad \frac{79.88}{183.5} \times \frac{Wx}{100} \text{ gms}$$

For Example : For a batch of 10 gms with composition 95wt% Al_2O_3 and 5wt% $SrTiO_3$

$$Al_2O_3 \text{ required} \quad \frac{10(100-5)}{100} \text{ gms}$$

$$9.5 \text{ gms}$$

$$SrCO_3 \text{ required} \quad \frac{147.62}{183.5} \times \frac{10 \times 5}{100}$$

$$= 0.4022 \text{ gms}$$

$$TiO_2 \text{ required} \quad \frac{79.88}{183.5} \times \frac{10 \times 5}{100}$$

$$= 0.217 \text{ gms}$$

Considering weight loss on ignition after dried powder . The amount of powder to be taken for preparing samples is given as below .

Suppose , x gms to be taken for one batch from a particular powder .

y% is the weight loss in that powder .

Then the amounts of powder should be taken = $\left(\frac{100}{100-y}\right).x$ gms

Example :

The weight loss on ignition after dried powder for Al_2O_3 is 0.36%

The amount of dried powder to be taken $=\left(\frac{100}{100-0.36}\right)(9.5)$

$=9.534$ gms

Appendix –B

Theoretical Density calculation of a mixed phase system .

The general formula used for a batch preparation is $(1-x)Al_2O_3 - xSrTiO_3$. Here 'x' is in weight fraction .

From standard data ,

Density of Al_2O_3 =3.987 gm/cm^3

Density of $SrTiO_3$ 5.12 gm/cm^3

For a 'w' gm batch with composition x wt% $SrTiO_3$.

Weight of Al_2O_3 $= \dfrac{w(100-x)}{100}$ gms

Weight of $SrTiO_3$ $= \dfrac{wx}{100}$ gms

Volume of Al_2O_3 $= \dfrac{w(100-x)}{100} \times \dfrac{1}{3.987}$ cm^3

Volume of $SrTiO_3$ $= \dfrac{wx}{100} \times \dfrac{1}{5.12}$ cm^3

Total volume $= \dfrac{w(100-x)}{100} \times \dfrac{1}{3.987} + \dfrac{wx}{100} \times \dfrac{1}{5.12}$

$$= \left(\frac{w(100-x)}{398.7} + \frac{wx}{512} \right) cm^3$$

$$= w\left(\frac{100-x}{398.7} + \frac{x}{512} \right) cm^3$$

Total weight $=$ w gms .

Theoretical Density $= \dfrac{\textit{Total weight}}{\textit{Total volume}}$

$$= \frac{w}{w\left(\frac{100-x}{398.7} + \frac{x}{512} \right)} \text{ gm/cm}^3$$

$$= \left(\frac{1}{\frac{100-x}{398.7} + \frac{x}{512}} \right) \text{gm/cm}^3$$

Example:

For 95 wt% Al_2O_3 and 5wt% $SrTiO_3$ composition .

$$\text{Theoretical Density} = \left(\frac{1}{\frac{100-5}{398.7} + \frac{5}{512}} \right) \text{gm/cm}^3$$

$$= 4.0316 \text{ gm/cm}^3$$

Similarly for other compositions can be calculated .

Appendix-C

Calculation of dielectric constant for $SrAl_{12}O_{19}$ phase from least square value .

The dielectric constant for $SrAl_{12}O_{19}$ phase was calculated from the measured dielectric constant , the 100% peak ratios for different phases from x-Ray diffractogram and the density .

The 100% peak ratios for different phases for different composition are given in the table below .

wt% $SrTiO_3$	ε_r measured	100% peaks in the obtained phases Al_2O_3: $SrTiO_3$: $SrAl_{12}O_{19}$	Density
1	10.52	80.5 : 2.4 :17.1	95.9
2	9.5	60.5 : 13.1 :26.4	92.62
5	9.91	30.4 : 23.2 : 46.4	95.45
8	9.45	69.6 : 8.7 :21.7	79.97

Taking 100% peak ratios for 1wt% $SrTiO_3$ composition .
Al_2O_3 : $SrTiO_3$: $SrAl_{12}O_{19}$ as 0.8050 : 0.0240 : 0.1710

For this composition the density is 95.9 .

Multiplying the above peak ratio with 0.959 ,we will get

0.772 : 0.023 : 0.1639

The dielectric constant for Al_2O_3 and $SrTiO_3$ are taken to be 10, 205 respectively .

The dielectric constant for this composition is 10.52 .

Now applying mixture rule ,

$\log\varepsilon = v_1\log\varepsilon_1 + v_2\log\varepsilon_2 + v_3\log\varepsilon_3$

$\log 10.52 = 0.772\log 10 + 0.023\log 205 + 0.1639\log\varepsilon_3$

ε_3 15.88 ~15.9

Similarly taking the peak ratios for other compositions the ε_r for $SrAl_{12}O_{19}$ can be calculated . which are given in the table below .

wt % $SrTiO_3$	ε_r of $SrAl_{12}O_{19}$
1	15.9
2	3.58
5	2.25
8	30.9

Now ε_r of $SrAl_{12}O_{19}$ phase varies from 2.25 to 30.9 . Taking different dielectric constant of $SrAl_{12}O_{19}$ phase between 2 and 30 , the dielectric constant for the samples for different compositions are recalculated . Taking measured value and calculated value of ε_r , $\sum(\varepsilon_{exp}-\varepsilon_{cal})^2$ values are calculated considering different ε_r of $SrAl_{12}O_{19}$ .which are given in table below . Then a graph is plotted between $\varepsilon_{SrAl_{12}O_{19}}$ and $\sum(\varepsilon_{exp}-\varepsilon_{cal})^2$ .From the graph corresponding to least square value , the ε_r of $SrAl_{12}O_{19}$ phase was noted .

TABLE :

$\varepsilon_{SrAl12O19}$	$\sum(\varepsilon_{exp}-\varepsilon_{cal})^2$
2	24.94
2.5	19.228
3.0	16.312

3.5	15.27
3.75	15.24
3.8125	15.288
3.875	15.36
4	15.58
6	26.08
8	45.148
10	69.0
12	95.8
14	124.68
16	155.16

From the graph the ε_r of $SrAl_{12}O_{19}$ comes out to be 3.67 .

Appendix-D

Calculation of TCF for $SrAl_{12}O_{19}$ phase from least square value .

The TCF of $SrAl_{12}O_{19}$ phase is also calculated by using the same procedure as described for the dielectric constant . The TCF of $SrAl_{12}O_{19}$ varies between -188.67 and -851.6 .Taking different values of $TCF_{SrAl_{12}O_{19}}$ between -188.67 and -851.6 , the TCF of the samples are recalculated . From measured and calculated values of TCF , the values of $\sum(TCF_{mea}-TCF_{cal})^2$ are calculated .These values are given in the table below .

TABLE:

$TCF_{SrAl_{12}O_{19}}$	$\Sigma(TCF_{mea}-TCF_{cal})^2$
-100	116365.15
-200	105711.9
-300	75011.82
-400	50543.7
-500	32337.0
-600	19208.27
-700	14611.5
-750	14047.2
-800	15050.44
-900	21720.85

From this graph corresponding to least square value, the TCF of $SrAl_{12}O_{19}$ phase was calculated .The TCF of $SrAl_{12}O_{19}$ phase comes to be –750 ppm/°C .

Appendix E

Software for lattice parameter calculation.

Lattice parameter calculation for Cubic system

```
#include<stdio.h>
#include<math.h>
#define lambda 1.54056
#define pi 3.1416

main()
{
float theta[50],h[50],k[50],l[50],a,t,d,b,g,cs_sq;
float sum_x,sum_xx,sum_y,sum_yy,sum_xy;
float m_a,c_y;
int i=0,n=0;
char ifile[10],ofile[10];
FILE *fpt, *spt;

system("clear");
printf("                    LATTICE PARAMETER CALCULATION FOR CUBIC SYSTEM
");
printf("\n\n\n\n\n\n\n\n");
printf("                             Enter Data File Name: ");
scanf("%s",&ifile);
fpt = fopen(ifile,"r");
  if(fpt == 0){
    printf("The File %s Does Not Exist In The Current
Directory\n\n\n",ifile);
    exit();
    }
sprintf(ofile,"%s.cbc",ifile);
spt = fopen(ofile,"w");
while(fscanf(fpt,"%f %f %f %f",&theta[n],&h[n],&k[n],&l[n])!=EOF)
  {
    n++;
  }
printf("\n                                 No. of Data = %d\n\n",n);
 fprintf(spt," RESULTS OF CUBIC SYSTEM FOR THE INPUT FILE \"%s\"\n
\n",ifile);
 fprintf(spt,"2(theta)        Cos^2(theta)        a  \n");
  sum_x=0;
  sum_xx=0;
  sum_y=0;
```

```
    sum_yy=0;
    sum_xy=0;


     for(i=0;i<=n-1;i++)
         {
           t=(pi/180)*(theta[i]/2);
         b=lambda/(sin(t)*2);
         g=(h[i]*h[i]+k[i]*k[i]+l[i]*l[i]);
         a=b*sqrt(g);
         if(i==0)
           d=a;
           cs_sq=cos(t)*cos(t);
         sum_x=sum_x+cs_sq;
         sum_xx=sum_xx+cs_sq*cs_sq;
         sum_y=sum_y+a;
       sum_yy=sum_yy+a*a;
      sum_xy=sum_xy+cs_sq*a;

         fprintf(spt,"\n%5.5f %15.5f %15.5f ",theta[i],cs_sq,a);
       }
      m_a=(sum_xy-(sum_x*sum_y/(float)n))/(sum_xx-
 (sum_x*sum_x/(float)n));
                c_y=(sum_y/n)-m_a*(sum_x/(float)n);

      printf("\n                                          a = %f  \n",c_y);
      fprintf(spt,"\n\n After Extrapolation (cos sq. theta = 0) a = %f
 \n",c_y);
  fclose(fpt);
  fclose(spt);
  printf("\n                                 Results Available In %s
 \n\n\n",ofile);
  printf("                                      Thank You\n\n\n\n");

  }
```

Lattice parameter calculation for Hexagonal System

```
#include<stdio.h>
#include<math.h>
#define lambda 1.54056
#define pi 3.1416
#define iteration 20

main()
{
float theta[50],h[50],k[50],l[50],a,c,c_a;
```

```
float sum_x,sum_xx,sum_y,sum_yy,sum_z,sum_zz,sum_xy,sum_xz,t,b,g,cs_sq;
float m_a,m_c,c_y,c_z,p,q,a1,a2,b1,b2,d1,d2;
int i=0,j=0,n=0;
char ifile[10],ofile[10];
FILE *fpt, *spt;
system("clear");
printf("                    LATTICE PARAMETER CALCULATION FOR HEXAGONAL SYSTEM
");
printf("\n\n\n\n\n\n\n\n");
printf("                                   Enter Data File Name: ");
scanf("%s",&ifile);
fpt = fopen(ifile,"r");
  if(fpt == 0){
    printf("The File %s Does Not Exist In The Current
Directory\n\n\n",ifile);
    exit();
    }
sprintf(ofile,"%s.hex",ifile);
spt = fopen(ofile,"w");
while(fscanf(fpt,"%f %f %f %f",&theta[n],&h[n],&k[n],&l[n])!=EOF)
  {
    n++;
  }
printf("\n         No. of Data=%d\n\n\n",n);
/*Initial c/a calculation*/
p=sin(pi/180*theta[0]/2);
q=sin(pi/180*theta[1]/2);
a1=p*p/(lambda*lambda);
a2=q*q/(lambda*lambda);
d1=l[0]*l[0]/4;
d2=l[1]*l[1]/4;
b1=(h[0]*h[0]+h[0]*k[0]+k[0]*k[0])/3;
b2=(h[1]*h[1]+h[1]*k[1]+k[1]*k[1])/3;
c_a=sqrt((a1*d2-a2*d1)/(a2*b1-a1*b2));

fprintf(spt,"LATTICE PARAMETER CALCULATION OF HEXAGONAL SYSTEM FOR THE
INPUT FILE \"%s\"\n\n",ifile);
printf("Initial value of c/a = %f\n\n",c_a);
fprintf(spt,"Initial value of c/a = %f\n\n",c_a);

for(j=0;j<iteration;j++)
  {
    sum_x=0;
    sum_xx=0;
    sum_y=0;
    sum_yy=0;
    sum_z=0;
    sum_zz=0;
    sum_xz=0;
    sum_xy=0;
    fprintf(spt,"Iteration No:%d\n\n",(j+1));
    printf("Iteration No:%d\n",(j+1));
```

```
    fprintf(spt,"2(theta)          Cos^2(theta)         a
c\n");

   for(i=0;i<=n-1;i++)
        {
           t=(pi/180)*(theta[i]/2);
        b=lambda/sin(t);
        g=(h[i]*h[i]+h[i]*k[i]+k[i]*k[i])/3;
        a=b*sqrt(g+(l[i]*l[i])/(4*c_a*c_a));
        c=b*sqrt(g*(c_a*c_a)+(l[i]*l[i]/4));
           cs_sq=cos(t)*cos(t);
        sum_x=sum_x+cs_sq;
        sum_xx=sum_xx+cs_sq*cs_sq;
        sum_y=sum_y+a;
        sum_yy=sum_yy+a*a;
        sum_z=sum_z+c;
        sum_zz=sum_zz+c*c;
        sum_xy=sum_xy+cs_sq*a;
        sum_xz=sum_xz+cs_sq*c;
        fprintf(spt,"\n%5.5f %15.5f %15.5f %15.5f",theta[i],cs_sq,a,c);
      }
     m_a=(sum_xy-(sum_x*sum_y/(float)n))/(sum_xx-
(sum_x*sum_x/(float)n));
     m_c=(sum_xz-(sum_x*sum_z/(float)n))/(sum_xx-
(sum_x*sum_x/(float)n));
     c_y=(sum_y/n)-m_a*(sum_x/(float)n);
     c_z=(sum_z/n)-m_c*(sum_x/(float)n);
     c_a=c_z/c_y;
     fprintf(spt,"\n\n          a = %f   c = %f   c/a =
%f\n\n\n",c_y,c_z,c_a);
     printf("\n a = %f   c = %f   c/a = %f\n\n\n",c_y,c_z,c_a);
  }
  fclose(fpt);
  fclose(spt);
  printf("\n                Results Available In %s \n\n\n",ofile);
  printf("                            Thank You\n\n\n\n");

  }
```

Lattice parameter Calculation for Rhombhohedral System

```
#include<stdio.h>
#include<math.h>
#define lambda 1.54056
#define pi 3.1416
#define iteration  20

main()
```

```
{
float theta[50],h[50],k[50],l[50],a,c,c_a,alpha;
float sum_x,sum_xx,sum_y,sum_yy,sum_z,sum_zz,sum_xy,sum_xz,t,b,g,cs_sq;
float m_a,m_c,c_y,c_z,p,q,a1,a2,b1,b2,d1,d2;
int i=0,j=0,n=0;
char ifile[10],ofile[10];
FILE *fpt, *spt;
system("clear");
printf("                    LATTICE PARAMETER CALCULATION FOR RHOMBHOHEDRAL
SYSTEM ");
printf("\n\n\n\n\n\n\n\n");
printf("                                   Enter Data File Name: ");
scanf("%s",&ifile);
fpt = fopen(ifile,"r");
  if(fpt == 0){
    printf("The File %s Does Not Exist In The Current
Directory\n\n\n",ifile);
    exit();
    }
sprintf(ofile,"%s.rom",ifile);
spt = fopen(ofile,"w");
while(fscanf(fpt,"%f %f %f %f",&theta[n],&h[n],&k[n],&l[n])!=EOF)
  {
    n++;
  }
printf("\n        No. of Data=%d\n\n\n",n);
/*Initial c/a calculation*/
p=sin(pi/180*theta[0]/2);
q=sin(pi/180*theta[1]/2);
a1=p*p/(lambda*lambda);
a2=q*q/(lambda*lambda);
d1=l[0]*l[0]/4;
d2=l[1]*l[1]/4;
b1=(h[0]*h[0]+h[0]*k[0]+k[0]*k[0])/3;
b2=(h[1]*h[1]+h[1]*k[1]+k[1]*k[1])/3;
c_a=sqrt((a1*d2-a2*d1)/(a2*b1-a1*b2));

fprintf(spt,"LATTICE PARAMETER CALCULATION OF ROMBHOHEDRAL SYSTEM FOR
THE INPUT FILE \"%s\"\n\n",ifile);
printf("Initial value of c/a = %f\n\n",c_a);
fprintf(spt,"Initial value of c/a = %f\n\n",c_a);

for(j=0;j<iteration;j++)
  {
    sum_x=0;
    sum_xx=0;
    sum_y=0;
    sum_yy=0;
    sum_z=0;
    sum_zz=0;
    sum_xz=0;
    sum_xy=0;
```

```
    fprintf(spt,"Iteration No:%d\n\n",(j+1));
    printf("Iteration No:%d\n",(j+1));
    fprintf(spt,"2(theta)          Cos^2(theta)          a
c\n");

   for(i=0;i<=n-1;i++)
       {
          t=(pi/180)*(theta[i]/2);
       b=lambda/sin(t);
       g=(h[i]*h[i]+h[i]*k[i]+k[i]*k[i])/3;
       a=b*sqrt(g+(l[i]*l[i])/(4*c_a*c_a));
       c=b*sqrt(g*(c_a*c_a)+(l[i]*l[i]/4));
          cs_sq=cos(t)*cos(t);
       sum_x=sum_x+cs_sq;
       sum_xx=sum_xx+cs_sq*cs_sq;
       sum_y=sum_y+a;
       sum_yy=sum_yy+a*a;
       sum_z=sum_z+c;
       sum_zz=sum_zz+c*c;
       sum_xy=sum_xy+cs_sq*a;
       sum_xz=sum_xz+cs_sq*c;
       fprintf(spt,"\n%5.5f %15.5f %15.5f %15.5f",theta[i],cs_sq,a,c);
     }
     m_a=(sum_xy-(sum_x*sum_y/(float)n))/(sum_xx-
(sum_x*sum_x/(float)n));
     m_c=(sum_xz-(sum_x*sum_z/(float)n))/(sum_xx-
(sum_x*sum_x/(float)n));
     c_y=(sum_y/n)-m_a*(sum_x/(float)n);
     c_z=(sum_z/n)-m_c*(sum_x/(float)n);
     c_a=c_z/c_y;
     fprintf(spt,"\n\n          a = %f  c = %f  c/a =
%f\n\n\n",c_y,c_z,c_a);
     printf("\n a = %f   c = %f   c/a = %f\n\n\n",c_y,c_z,c_a);

 }
     a=sqrt(3*c_y*c_y+c_z*c_z)/3;
     alpha=180/pi*2*asin(3/(2*sqrt(3+((c_z*c_z)/(c_y*c_y)))));
     fprintf(spt,"\n\nFor Rhombohedral System...");
     fprintf(spt,"\n\n          a = %f        alpha = %f
degree\n\n\n",a,alpha);
     printf("\n\nFor Rhombohedral System...");
     printf("\n\n          a = %f        alpha = %f
degree\n\n\n",a,alpha);
 fclose(fpt);
 fclose(spt);
 printf("\n               Results Available In %s \n\n\n",ofile);
 printf("                             Thank You\n\n\n\n");

 }
```

A 130825